Synthesis and Structural Characterization of Nickel encapsulated Carbon nanotubes

A Major Project dissertation submitted

in partial fulfillment of the requirement for the degree of

Master of Technology

In

Nanoscience and Technology

Submitted by

Rajesh Kumar
(2K13/NST/09)
Delhi Technological University, Delhi, India

Under the supervision of

Dr. Pawan K Tyagi

Department of Applied Physics
Delhi Technological University
(Formerly Delhi College of Engineering)
Shahbad Daulatpur, Main Bawana Road, Delhi-110042, INDIA

CERTIFICATE

This is to certify that the M. Tech. dissertation entitled **"Synthesis and Structural Characterization of Nickel encapsulated Carbon nanotubes"**, submitted by **Rajesh Kumar (2K13/NST/09)** in partial fulfillment of the requirement for the award of the degree of Master of Technology, Delhi Technological University (Formerly Delhi College of Engineering, University of Delhi), is an authentic record of the candidate's own work carried out by him under my guidance.

The information and data enclosed in this dissertation is original and has not been submitted elsewhere for honouring of any other degree.

Date: 29 /07/2015

Dr. Pawan Kr. Tyagi
Assistant Professor,
(Project Guide)
Dept. of Applied Physics
Delhi Technological University

Dr. S. C. Sharma
Professor and HOD,
Dept. of Applied Physics
Delhi Technological University

CANDIDATE DECLARATION

I, Rajesh Kumar, Roll No.-2K13/NST/09, student of M. Tech. (NANO SCIENCE AND TECHNOLOGY), hereby declare that the dissertation/project titled **"Synthesis and Structural Characterization of Nickel Encapsulated Carbon nanotubes"** under the supervision of Dr. Pawan Kumar Tyagi, Department of Applied Physics, Delhi Technological University, in partial fulfilment of the requirement for the award of the degree of Master of Technology has not been submitted elsewhere for the award of any Degree.

Rajesh Kumar
M.Tech. (NST)
Dept. of Applied Physics
Delhi Technological University

ACKNOWLEDGEMENT

I take this opportunity to express my sincere gratitude to all those who have been instrumental in the successful completion of this project.

Dr.Pawan Kr. Tyagi, Assistant Professor, Dept. of Applied Physics, Delhi Technological University, my project guide, has guided me for successful completion of this project. It is worth mentioning that he always provides the necessary guidance and support.

I would like to express my sincere thanks to Ms. Reetu Kumari, Research Scholar, Dept of Applied Physics, Delhi Technological University, who has left no stone unturned in helping me throughout my project.

Also, I will be ever grateful to my fellow classmate, Ms. Nimisha Kakoty who has always been a source of inspiration and never failed to offer a helping hand in times of need.

I am grateful for the help and cooperation of our HOD Prof.S.C.Sharma.

To all the named and many unnamed, my sincere thanks. Surely it is almighty's grace to get things done fruitfully.

RAJESH KUMAR
2K13/NST/09
M.Tech. (NST)

Contents

List of figures

List of Abbreviations

VLSI	Very Large Scale Integration
Ar	Argon
CVD	Chemical Vapour Deposition
Si	Silicon
SCCM	Standard Cubic Centimeters per Minute
1D	One Dimensional
SEM	Scanning Electron Microscopy
XRD	X Ray Diffraction
H_2	Hydrogen
TEM	Transmission Electron Microscopy

List of Tables

ABSTRACT

The search for one dimensional materials to substitute silicon in electronic devices has widened up in the past decade. Carbon nanotube is a promising material as it boasts of its unique switching nature of conductivity from metallic to semiconducting according to its geometry. In this project, the goal is to design and implement an optimized method for the growth of Ni-encapsulated carbon nanotubes using thermal CVD and to characterize it using standard available characterization techniques.

1. Introduction

1.1 Carbon nanotubes

Carbon Nanotubes are long, thin cylinders of carbon, and were discovered in 1991 by Sumio Iijima. These are quite large macromolecules which are completely unique for their shape, remarkable physical properties and size, Their intriguing structures have initiated much excitement in the recent years and a substantial amount of research has been devoted to understand their entirety. Presently, the physical properties are still in the process of being discovered and disputed. The nanotubes have a very wide range of electronic, structural, and thermal properties which change according to the different types of nanotube (defined by its length, diameter, and twist, or chirality). In order to make things much more interesting, apart from possessing a single cylindrical wall (SWNTs), these nanotubes can possess multiple walls (MWNTs)—i.e., cylinders inside the inner cylinders.

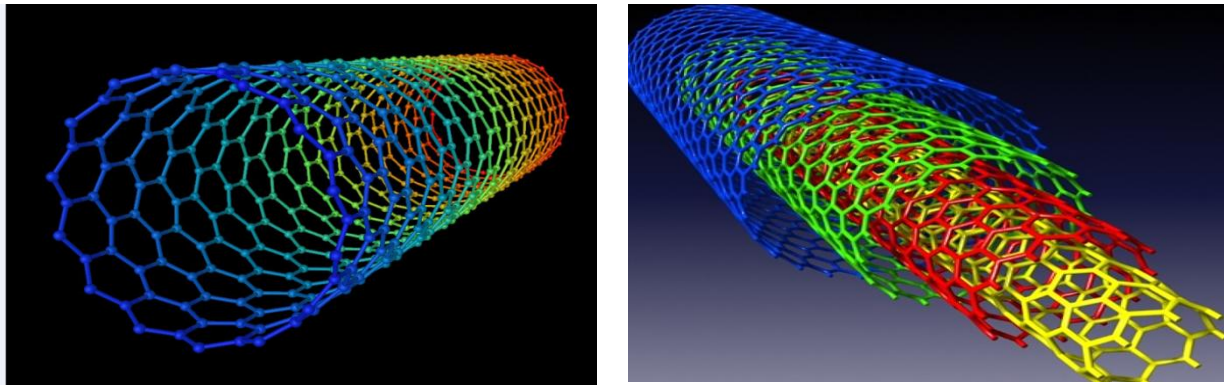

(a) **(b)**

Figure 1.1. Representation of CNT (a) Single walled CNT (b) Multi walled CNT[51]

It is comparatively easy to think of a single-walled carbon nanotube (SWNT). Ideally, it is sufficient to consider a perfectly formed graphene sheet (graphene is a monoatomic polyaromatic layer comprising of sp^2-hybridized carbon atoms that are arranged in hexagons; authentic graphite comprises of layers of this very graphene) and to roll it upto a cylinder such that hexagonal rings placed in contact coherently join. The tips of these tube are sealed by the two

caps, whereby each cap being hemi-fullerene of the required diameter. Three unique geometries of the carbon nanotubes are there which are referred to as flavors. These three flavors are zig-zag, armchair, and chiral [e.g. zig-zag (n, 0); armchair (n, n); as well as chiral (n, m)]. These details can be easily comprehended by the help of the figures below.

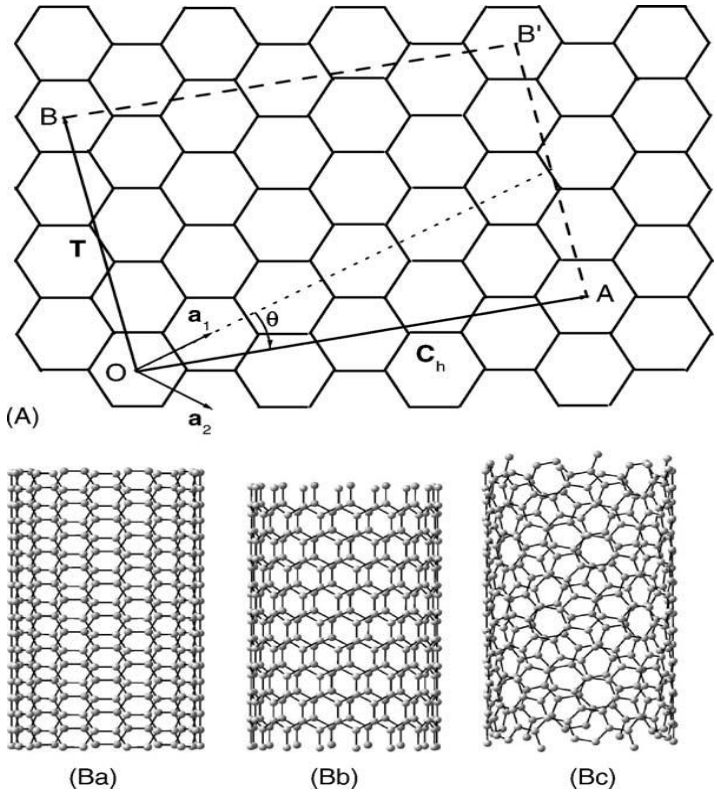

Figure 1.2 a-c Different ways of rolling a graphene sheet to form CNT[52]

By geometry, there is no restrain on the diameter of the tube. But calculations have indicated that collapsing this single-wall tubular structure into a flattened two-layered ribbon is energetically more favorable than to maintain this tubular morphology beyond a particular diameter value of about 2.5nm. On the other hand, it is well deducable that the shorter the radius of curvature is, the higher the energetic cost and the stress becomes, even though SWNTs having diameters as small as 0.4 nm have been already synthesized successfully. Therefore, the suitable energetic compromise is reached for about 1.4nm, the most repeated diameter encountered irrespective of the synthesis technique when the conditions which ensure high SWNT yields are utilized. There is no restrain on nanotube length, that depends only on the limitations of the method of preparation and the specific conditions that are used for the synthesis (residence time, thermal

gradients, and so on). Experimental data are found to be consistent with these statements, since these SWNTs wider than 2.5 nm are only rarely reported in the literature, whatever the preparation method, while the length of the SWNTs can be in the micrometer or the millimeter range. These special features make these single-wall carbon nanotubes an extremely unique example of single molecules possessing huge aspect ratios. Two important consequences derive from the SWNT structure as described above:

1. All the carbon atoms are involved in the hexagonal aromatic rings only and therefore are in equivalent positions, but except at each and every nanotube tip, where $6 \times 5 = 30$ atoms are found to be involved in pentagonal ring (considering that the adjacent pentagons are quite unlikely) – though neither more, nor less, as the consequence of Euler's rule which also governs the structure of fullerene. For ideal SWNTs, the chemical reactivity will thereby, be highly favoured at tube tips, at the pentagonal rings.

2. Although carbon atoms are found to be involved in the aromatic rings, the C=C bond angles are however not planar. This implies that the hybridization of those carbon atoms is certainly not pure sp^2; it does possess some degree of the sp^3 character, which is in inverse proportion to that tube radius of curvature. The effect is similar for C_{60} fullerene molecules, wherein the radius of curvature is 0.35 nm, and therefore whose bonds have 10% sp^3 character. This is believed, on the one hand, to make SWNT surface somewhat more reactive than the regular and planar graphene, inspite of it still consisting of aromatic ring faces. This somehow induces the variable overlapping of the energy bands, which results in versatile and unique electronic behavior. As illustrated by the above figure, there are multiple ways to roll a graphene into a single-walled nanotube, with some of the resultant nanotubes exhibiting planes of symmetry, both parallel as well as perpendicular to the nanotube axis (such as those SWNTs from Fig. 1-2a and b), and the others do not (such as the SWNT from the Fig. 1-2c). Just like the terms used for the molecules, the latter are commonly termed as *chiral* nanotubes, since they are not able to be superimposed on their very own image in a mirror. The various ways in order to roll graphene into tubes are thereby mathematically defined by vector of the helicity $\boldsymbol{C}h$, and angle of helicity θ.

1.2 History

Till the mid-1980's, graphite and diamond were thought to be the only two physical forms of pure solid carbon. Graphite and diamond have different properties and physical structures. Their

atoms however are arranged in covalently bonded network. These two physical forms of carbon atoms are termed as allotropes.

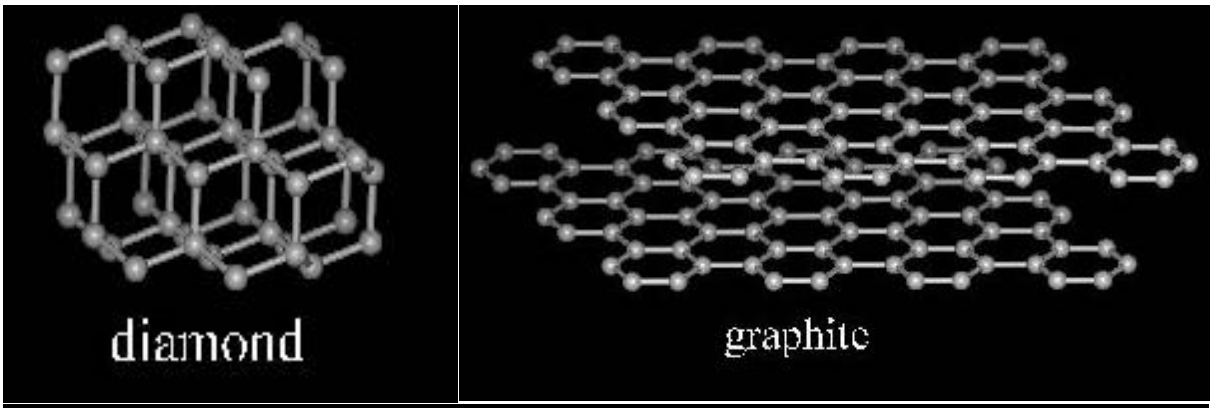

Figure 1.3. Allotropes of carbon[53]

In 1985, a group of researchers headed by Robert Curl and Richard Smalley of Rice University in Houston and Harry Kroto of Sussex University in England made an interesting discovery. With an strong pulse of laser light , they vaporized samples of graphite and they used a fine stream of helium gas in order to carry the vaporized carbon to the mass spectrometer. This mass spectra showed peaks relating to the clusters of carbon atoms, having a particularly intense peak corresponding to the molecules composed of the 60 carbon atoms, C_{60}.This fact that the C_{60} clusters were formed with such ease, led the research group to propose a novel form or allotrope of carbon had been just discovered. It is spherical shaped and formed the structure of a ball having 32 faces. Of these 32 faces, there are 12 pentagons and are 20 hexagons exactly like a soccer ball.

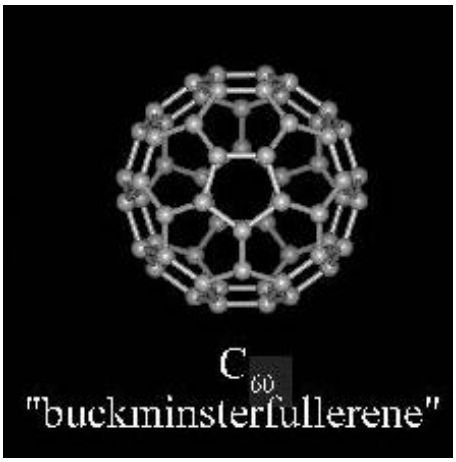

Figure 1.4. Bucky Ball[54]

After this tremendous discovery, a number of related molecules (C_{84}, C_{36}, C_{70}, and C_{76}) which comprises of carbon atoms only were discovered. They along with buckyball were recognized as a novel allotrope of carbon. This novel class of carbon molecules is termed as the fullerenes. The fullerenes comprises of pentagons and hexagons that form spherical shape. The fullerenes have been also proposed as possible HIV inhibitors and potential constituents in the interstellar space.

The interesting and unusual geometric properties of the new allotrope of carbon did not halt with these soccer shaped molecules. Moreover, it was discovered that the carbon atoms can undergo long cylindrical tube formation. Originally, these tubes were termed as "buckytubes". But nowadays they are better known as the carbon nanotubes or for short as CNT. These tubular shaped molecules can be imagined as a sheet of graphite that is rolled into tube.

1.3 Properties of carbon nanotubes

Electronic and Optical Properties: The electronic states in SWNTs are strongly influenced by their one-dimensional cylindrical structures. One-dimensional subbands are formed that have strong singularities in the density of states (Van Hove singularities). By rolling the graphene sheet to form a tube, new periodic boundary conditions are imposed on the electronic wavefunctions, which give rise to one-dimensional subbands: $CnK = 2q$ where q is an integer. Cn is the roll-up vector $na1+ma2$ which defines the helicity (chirality) and the diameter of the

tube. Much of the electronic band structure of CNTs can be derived from the electronic band structure of graphene by applying the periodic boundary conditions of the tube under consideration. The conduction and the valence bands of the graphene only touch at six corners (*K* points) of the Brillouin zone. However, if one of these subbands passes through the *K* point, then the nanotube is metallic; otherwise, it is certainly, semiconducting.

This is a unique property that is not found in many other one-dimensional system, which means that or certain orientations of the honeycomb lattice with respect to the tube axis (chirality), some nanotubes are semiconducting and others are metallic. The band gap for semiconducting tubes is found to be inversely proportional to the tube diameter. Knowing (*n*,*m*) allows us, in principle, to predict whether the tube is metallic or not. The energy gap decreases for larger tube diameters and MWNTs with larger diameter are found to have properties similar to other forms of regular, polyaromatic solids. It has been shown that electronic conduction mostly occurs through the external tube for MWNTs; even so, interactions with internal tubes often cannot be neglected and they depend upon the helicity of the neighboring tubes. The electronic and optical properties of the tubes are considerably influenced by the environment. Under externally applied pressure, the small interaction between the tube walls results in the internal tubes experiencing reduced pressure. The electronic transition energies are in the infrared and visible spectral range. The one-dimensional Van Hove singularities have a large influence on the optical properties of CNTs.

Mechanical properties: While tubular nanomorphology is also observed for many two-dimensional solids, carbon nanotubes are unique due to the particularly strong bonding between the carbons (sp^2 hybridization of the atomic orbitals) of the curved graphene sheet, which is stronger than in diamond (sp^3 hybridization), as showed by the difference in the C−C bond lengths (0.142 versus 0.154 nm for graphene and diamond respectively). This makes carbon nanotubes – SWNTs or c-MWNTs – particularly stable against deformations. Tensile strength of the SWNTs can be 20 times that of steel and has actually been measured as ≈ 45 GPa. Very high tensile strength values are also expected for ideal (defect-free) c-MWNTs, since combining perfect tubes concentrically is not supposed to be detrimental to the overall strength of tube, provided that the tube ends are well capped (or else, concentric tubes could glide relative to each

other, inducing high strain). Tensile strength values as high as ≈ 150 GPa have actually been measured for perfect MWNTs from an electric arc, although the reason for such a high value compared to that measured for SWNTs is not clear. It probably reveals the difficulties involved in carrying out such measurements in a reliable manner. The flexural modulus of perfect MWNTs should logically be higher than that for SWNTs, with a flexibility that decreases as the number of walls increases. On the other hand, measurements performed on defective MWNTs obtained from CCVD exhibit a range of 3–30 GPa. Values of tensile modulus are also the highest values known, 1 TPa for MWNTs, and possibly even higher for SWNTs, up to 1.3 TPa.

1.4 Applications of Carbon Nanotubes

This unique material exhibits the characteristics to be suitable for a long list of applications. However, only a few of them have been mentioned below.

Because of the carbon nanotube's superior mechanical properties, many structures have been proposed ranging from everyday items like clothes and sports gear to combat jackets and space elevators.

Because of the high mechanical strength of carbon nanotubes, research is being made into weaving them into clothes to create stab-proof and bulletproof clothing. The nanotubes would effectively stop the bullet from penetrating the body, although the bullet's kinetic energy would likely cause broken bones and internal bleeding.

Nanotube-based transistors, also known as carbon nanotube field-effect transistors (CNTFETs), have been made that operate at room temperature and that are capable of digital switching using a single electron. However, one major obstacle to realization of nanotubes has been the lack of technology for mass production.

One of the promising applications of single-walled carbon nanotubes (SWNTs) is their use in solar panels, due to their strong UV/Vis-NIR absorption characteristics. Research has shown that they can provide a sizable increase in efficiency, even at their current unoptimized state. Solar cells developed at the New Jersey Institute of Technology use a carbon nanotube complex,

formed by a mixture of carbon nanotubes and carbon buckyballs (known as fullerenes) to form snake-like structures. Buckyballs trap electrons, but they can't make electrons flow. When sunlight is added to excite the polymers, the buckyballs would grab the electrons. Nanotubes, behaving like copper wires, will then be able to make the electrons or current flow.

In addition to being able to store electrical energy, there has been some research in using carbon nanotubes to store hydrogen to be used as a fuel source. By taking advantage of the capillary effects of the small carbon nanotubes, it is possible to condense gases in high density inside single-walled nanotubes. This allows for gases, most notably hydrogen (H_2), to be stored at high densities without being condensed into a liquid. Potentially, this storage method could be used on vehicles in place of gas fuel tanks for a hydrogen-powered car. A current issue regarding hydrogen-powered vehicles is the on-board storage of the fuel. Current storage methods involve cooling and condensing the H_2gas to a liquid state for storage which causes a loss of potential energy (25–45%) when compared to the energy associated with the gaseous state. Storage using SWNTs would allow one to keep the H2 in its gaseous state, thereby increasing the storage efficiency.

1.5 Filled Carbon Nanotubes

The unique mechanical and electrical properties of the sp^2 -hybridized molecular nanostructures are the reason for making them one of the most potential building blocks for nanotechnology. They possess large aspect ratio, small size, exceptional high Young's modulus and ballistic transport properties. In addition to these exceptional properties, CNTs can be opened and filled without any effect on their stability and have chemically strongly stable carbon shells. They can be filled with therapeutics, metals, salts, semiconductors, organic materials etc., either during the time of synthesis (Fe, Co, Ni) or subsequently through opening, filling and closing of these CNT. Their crystalline carbon shells protect those filling material from the oxidation, or the environment or may be, against each other. Hence, they are considered as safe and smart carrier systems in nanoscale that can be encapsulated with tailored materials in order to address certain purposes. These are filled or encapsulated Carbon Nanotubes.

The study of these ferromagnetic-encapsulated carbon nanotubes is not only interesting due to the strong potential applications, but also from a scientific viewpoint. Compared to the bulk material, these encapsulated metal nanowires most often exhibit new magnetic and structural properties, that originates from large geometric aspect ratio and their low dimensionality. In fact, their internal cavity may easily serve as an ideal nanoscale crucible for the conduction of metallurgical operations at nanoscale with iron or any other metals. Thus, the range of interests has varied between the strong influence of the effects of the carbon nanotubes confinement on structure of the metal phases, on phase distribution as well as phase transformation (in case of iron, the stability of the bodycentered cubic (bcc)-Fe, the face-centered cubic (fcc)-Fe, and Fe_3C – or any other higher carbides – can vary), and finally on the variation of physical (magnetic) properties.

The new combination of the magnetic materials and the CNTs is soon rising to be a very interesting area of the advanced research. These CNTs are famous to be ballistic one-dimensional conductors. This implies that they are capable of transmission of electron over very long distances. The spin dependent transport effects associated with the high magneto-resistance values are displayed vehemently by these ferromagnetically contacted CNTs. They are encapsulated with ferromagnetic materials, such as Fe, Ni or Co, and hence, can be used as nano-magnets and they can have important applications in the high density magnetic data storage.

Metallocenes

A metallocene is typically a compound comprising of two cyclopentadienyl anions (Cp, that is $C_5H_5^-$) bound to the metal center (M) in oxidation state II, alongwith the resulting general formula being $(C_5H_5)_2M$. Very closely related to metallocenes are the metallocene derivatives, for example, vanadocene dichloride, titanocene dichloride. Some metallocenes and their derivatives are found to exhibit catalytic properties, even though metallocenes are very rarely used industrially. The cationic group 4 metallocene derivatives are related to the $[Cp_2ZrCH_3]^+$ catalyze olefin polymerization. The metallocenes are the subset of a broader class of the organometallic compoundsthat are termed as the sandwich compounds.

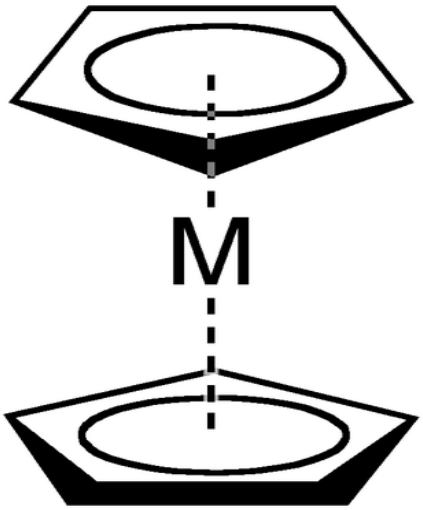

Figure 1.5. Representation of metallocene[55]

History: The first metallocene that was be classified was the ferrocene, and it was discovered simultaneously by Keally and Pauson and also, Miller in 1951. Keally and Pauson attempted to synthesize fulvalene by the oxidation of cyclopentadienyl salt with the anhydrated $FeCl_3$ but instead, they obtained the substance $C_{10}H_{10}F$. At the same time, it was reported that Miller synthesized the same iron product through a reaction of cyclopentadiene with the iron in presence of potassium, aluminum, or molybdenum oxides. Wilkinson as well as Fischer determined the structure of the "$C_{10}H_{10}Fe$" and they were awarded the Nobel Prize in 1973 in Chemistry for their great work on sandwich compounds, which included structural determination of ferrocene. It was they who determined that carbon atoms of cyclopentadienyl (Cp) ligand strongly contributed equally to bonding and this bonding occurred because of the metal d-orbitals and also, the π-electrons in p-orbitals of those Cp ligands. This complex is now termed as ferrocene and this group of transition metaldicyclopentadienyl compounds is termed as metallocenes and they have the general formula $[(\eta^5\text{-}C_5H_5)_2M]$. Fischer prepared the ferrocene derivatives involving Co and Ni first amongst all. Most often derived from the substituted derivatives of cyclopentadienide, the metallocenes of many such elements have been prepared.

Definition: General name "metallocene" is derived from the term " ferrocene", Cp_2Fe or $(C_5H_5)_2Fe$, named systematically bis(η^5-cyclopentadienyl)iron(II). According

to IUPAC definition, any metallocene contains a transition metal alongwith two cyclopentadienyl ligands that are coordinated in a sandwich structure, i. e., these two cyclopentadienyl anions are on the parallel planes with equal bond strengths and lengths. With the use of the nomenclature of "hapticity", equivalent bonding of all these 5 carbon atoms of cyclopentadienyl ring is termed as η^5, and pronounced "pentahapto".However, there are exceptions, like, uranocene, that has two cyclooctatetraene rings which are sandwiching one uranium atom.

In the metallocene names, the prefix before the **-ocene** ending indicates at the metallic element that is present between the specific Cp groups. For instance, in the ferrocene, iron(II), ferrous iron is present.

Nickelocene

The Nickelocene is organonickel compound having the formula $Ni(\eta^5\text{-}C_5H_5)_2$. It is also termed as bis(cyclopentadienyl)nickel or $NiCp_2$. It is a bright green paramagnetic solid and is of persisting academic interest, even although it has yet no practical applications.

Structure and Bonding: $Ni(C_5H_5)_2$ belongs to the group of the organometallic compounds known as the metallocenes. These metallocenes usually adopt structures wherein a metal ion is found to be sandwiched between the two parallel cyclopentadienyl (Cp) rings. The structure is quite relevant to the solubility in the organic solvents and also, volatility. In solid-state, this molecule has the D_{5h} symmetry, in which the two rings are eclipsed.

Ni center has the formal 2+ charge, while, Cp rings are assigned usually as the cyclopentadienyl anions (Cp^-), that are related to the cyclopentadiene by the deprotonation. The structure is thus, similar to the ferrocene. In the terms of its electronic structure, the three pairs of d electrons on the nickel are allocated to three d orbitals that are involved in the Ni - Cp bonding: d_{xy}, $d_{x^2-y^2}$, d_{z^2}.Out of the remaining two, one d-electrons is placed in each of d_{yz} and d_{xz} orbitals, that gives rise to this molecule's paramagnetism, as observed in the exceptionally high field chemical shift that is observed in its H NMR spectrum. With some 20 valence electrons, the nickelocene has the highest electron count, out of the transition metal metallocenes. However, the cobaltocene,

$Co(C_5H_5)_2$, having only 19 valence electrons is a stronger reducing agent, that illustrates the fact that the energy of electron, not electron count determines the redox potential.

1.6 Properties of filled CNTs

Magnetic Properties: Typical hysteresis loops were measured for the filled carbon nanotube carpet on the precoated silicon substrate. The measurements always reveal a uniaxial magnetic anisotropy with the easy axis along the tube axis. Saturation magnetization M_{sat} and coercivity HC are dependent not only on the ferromagnetic bcc-iron fraction, but also on the alignment level, and diameter and length of the filled carbon nanotubes on the substrate. For example, the higher the growth rates, the stronger is the alignment; magnetic anisotropy also increases with increasing lengths. This means the aspect ratio determines the magnetic anisotropy (so-called shape anisotropy). Moreover, it should be noted that values of coercivity reached are far higher than for the bulk material (max. HC(Fe) in Fe-filled tube carpets = 130 mT, compared to bulk HC(Fe) = 0.009 mT). With an increase in the growth temperature the diameter of the encapsulated Fe nanowires becomes larger. This effect decreases the coercivity, the magnetic hardness, and hence, reduces the magnetic anisotropy. As shown here, dependence on the parameters of the growth process can strongly affect the magnetic properties. The most important variables are the growth temperature and the sublimation temperature of ferrocene, because these parameters strongly affect the diameters, lengths, and alignment of the nanotubes.

Electronic Properties: CNTs have been found to be very good field emitters with low turn – on fields and high current densities. This has made them attractive as possible electron sources in, for instance, electron microscopes and cathode ray oscilloscopes. It has been found that arrays of CNTs filled with iron oxide has a lower turn-on field than unfilled CNTs.

Numerous studies have been conducted till date on the field emission from standard unfilled CNTs that have linked the field emission properties of the CNTs to their structural properties. However, there is very little data available on the field emission properties of filled CNTs, particularly individual filled CNTs.

1.7 Applications of filled CNTs

The structures of the nanotubes may imagined as metal nanomagnets or nanowires within the carbon nanotubes. These nanowires are strongly protected by encapsulation against the oxidation and most other chemical reactions and influences. Thus, such nanowires exhibit long-term stability. Hence, this is a magnanimous advantage compared to uncoated, pure nanowires, and thus, opens new application fields.

These ferromagnetic-filled carbon nanotubes find applications ranging from the magnetic data-storage devices, to the implementation of individual filled tubes in any sensor system for the magnetic force microscopy.

Another probable utility of filled carbon nanotubes is observed in the field of biomedicine as ferromagnetic nanocontainers initiating a novel antitumour therapeutic concept in treatment of the cancer disease.

Furthermore, exceptional electronic properties and hollow structure characteristic of these CNTs could have a significant potential for the use of these magnetic nanotubes in many other applications which ranges from electromagnetic devices to the magnetically guided drug delivery system. The filled carbon nanotubes represent a befitting material for the magnetically guided hyperthermia and, also, functionalized inside and outside the tube, a very unique drug delivery/carrier system.

1.8 Growth mechanism of filled CNTs

Analysing the growth mechanisms of the carbon nanotubes is a prime requisite for the desired synthesis to obtain certain special properties that are needed for the desired applications. Up to now there is no generally accepted growth mechanism and further research is necessary. The knowledge and understanding of the mechanism is under continuing development and several modifications were discussed during the last two decades. A few widely discussed mechanisms are mentioned below:

VLS mechanism

The basis of all is the vapor-liquid-solid (VLS) mechanism which was originally developed for the growth of silicon whiskers by Wagner and Ellis. It consists of the assumption that a gaseous phase, a liquid phase and a solid interacts. The precursor is supplied as the gas. The liquid phase is liquified molten catalyst particle present on the solid substrate. During this growth process it is observed that the precursor decomposed in a specific area of the surface of the liquid particle at the temperature T1. The precursor material dissolves until saturation at concentration c1 is attained. It is assumed that this particle occupies an area with a lower temperature T2 and a lower concentration c2. Thus the presence of both a concentration and thermal gradient is assumed. Precursor materials diffuse through the particle and precipitates at T2. These very basic assumptions of the mechanism allow the application to other systems.

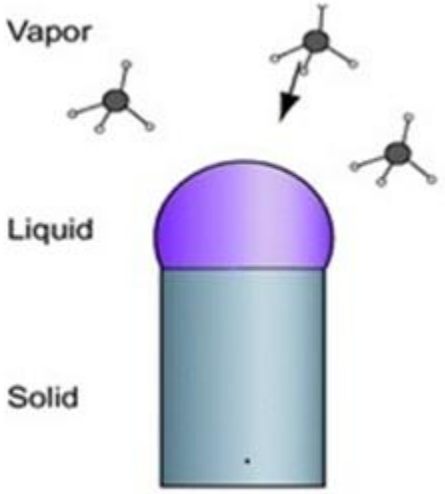

Figure 1.6. Representation of VLS mechanism[56]

Base and tip growth mode

This is one of the very first mechanism to explain growth of the carbon whiskers which was initially developed by Baker on basis of VLS mechanism. He and his group performed in-situ studies on growth of the carbon whiskers by employing controlled atmosphere electron microscopy (CAEM). During this formation, the liquified metal catalyst particles were either on tip or bottom of as-formed whiskers. Because of the forces acting on these catalyst particles, they

undergo deformation during the process which results in two different growth modes. If there is strong attractive interaction between catalyst and substrate, then a good wettability is found which lead to the contact angles below 90˚ and these particles are found to be most likely remains on the surface of substrate. Since decomposition of the hydrocarbons relies on catalytical activity of the particle surface which supplies carbon atoms can solely connect to already existing carbon structures present at the particle whisker interface. Thus, the oldest part of whisker is the tip while the youngest part is the bottom. This is why, it is termed as the base growth mode. On the other hand, if there is a repulsive interaction between particle and surface then, a contact angle more than 90˚ will be established. The particle then most likely detaches itself from the surface and lifts itself up. In this case, thus, the oldest part of CNT is nearest to the substrate surface while the youngest part is tip. Thus, this is termed as the tip growth mode.

In the figure 1.7, it is showed that the metal particles on the surface are exposed to gaseous hydrocarbons, which decompose catalytically on the surface of the catalyst particle. An exothermic decomposition is assumed and a carbon concentration as well as a temperature gradient form. After its decomposition the carbon diffuses from the hot area with a higher concentration to the colder region of the particle and precipitates to form the graphitic structure of the CNT wall. The particle remains attached to the substrate.

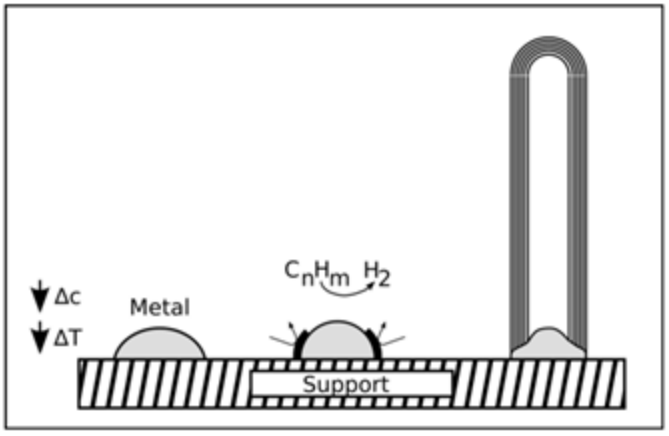

Figure 1.7. Base Growth Mode[57]

In the figure 1.8, it is showed that the metal particle is only weakly bound to the substrate surface. The decomposition of the hydrocarbons takes place at the upper side of the particle. Again an exothermic decomposition is assumed and the temperature and carbon concentration increases at the top of the particle which gets deformed during this process and detaches from the

substrate. The carbon now diffuses to the colder side of the particle and precipitates to form the CNT shells.

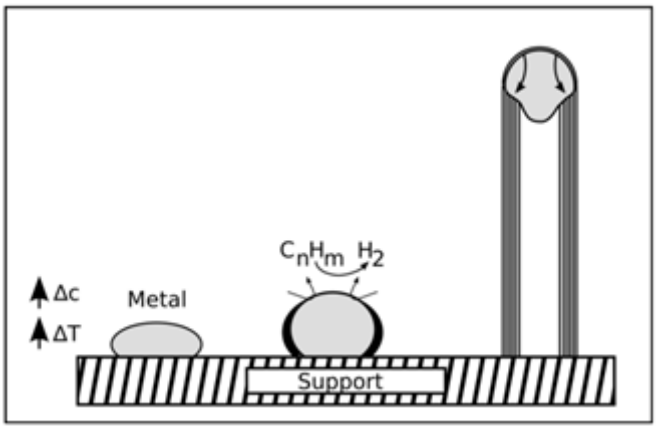

Figure 1.8. Tip Growth Mode[58]

Base and tip growth mode for filled CNT

For filled CNT, not only the formation of the carbon shells but also the formation of the in-situ filling has to be explained. However, it is specifically difficult to describe the influence of the catalyst because it is applied on the substrate and additionally as floating catalyst from the decomposed precursor. During the whole growth process metal particles, mostly catalytically active, do interact with the forming CNT. Nevertheless, several groups adjusted the VLS mechanism and the concepts of the tip and base growth mode to explain the formation of in-situ filled CNT. From the experiments carried out by Zhang indicated a growth mechanism that could easily explain the in-situ filling of carbon nanotubes with iron during synthesis. This scheme of the mechanism is thus shown in Figure 1.9. The figure presents the growth process of in-situ filled CNT. (A) shows the slow growth stage. The carbon shells at the open tip react with carbon clusters from the gas phase. In (B) a larger catalyst particle attaches to the open tip and the fast growth stage starts. The CNT grows fast and the pressure caused by the shells deforms the catalyst particle. In this stage (C) a filling section is formed. If the supply with catalyst material stops the slow growth stage continues.

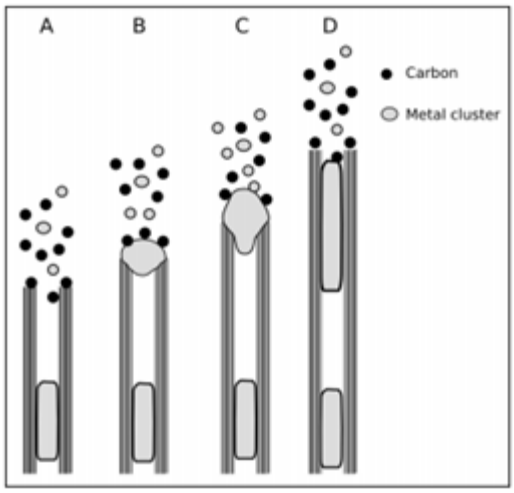

Figure 1.9. Base and tip growth mode[59]

Combined growth mode

An intensive discussion and interesting approach to explain the growth of metal-filled CNT was presented by Kunadian. They combined tip- growth and base-growth mode explaining the formation of the filling in the context of a closed tip growth process (compare Figure 12(B)). In the continuous-feed CVD the precursor containing both the carbon source and the catalyst material is provided continuously during the process. In the mechanism (Figure 14) it is assumed that the initial state follows the base growth mode. Hydrocarbons decompose on the surface of these catalyst particles. Because of the floating catalyst conditions metal clusters are formed and hydrocarbons can also decompose already in the gas phase. The catalytically active metal clusters and the carbon atoms fall onto the catalyst particles which remain anchored to the surface of substrate. It may be assumed that this results in a continuing change in catalyst conditions. Each and every cluster that connects to catalyst particle modifies the volume, shape and the carbon concentration of the catalyst. Thus under these floating catalyst conditions it is very likely that the growth mode switches from the base to tip growth mode. After the switching takes place, the filling process and also, the shell formation occurs simultaneously at the tip.

Figure 1-10 gives the steps of the combined growth mechanism. In step A a catalyst particle is formed. Step B describes the decomposition of hydrocarbons on the particle surface. Due to the floating catalyst method catalytic processes occur also in the gas phase forming metal and carbon clusters. In step C the deposition of iron particles at the growing site takes place continuously,

thereby the growth mode changes from base to tip growth mode (step C-D). When further material deposits from the gas phase the growth continues (step E) until a stable cap is formed. If the cap is closed so called secondary growth might occur. This is often tip growth since the wettability of the metal catalyst is low and the particles easily detach (step F and G).

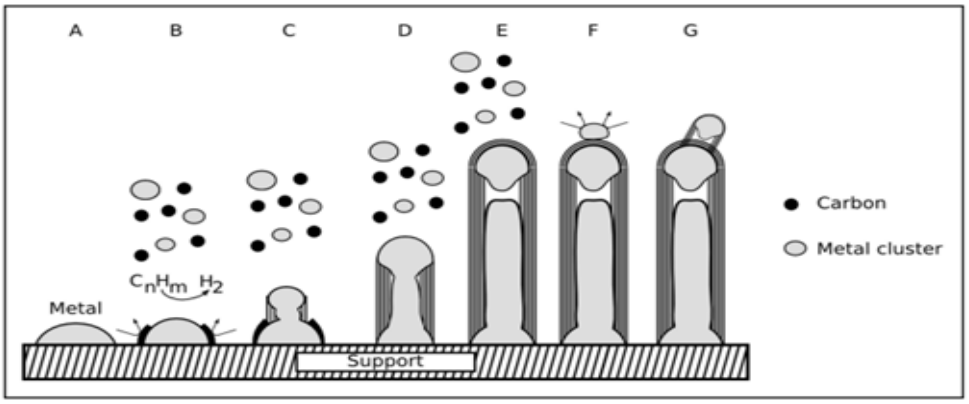

Figure 1.10. Combined Growth Mode[60]

2. Preferential Method Adopted for the Synthesis of Ni- filled Carbon Nanotubes

Basically the methods for the synthesis of empty and filled carbon nanotubes are similar. At both processes hydrocarbon precursor compounds are required which deliver the carbon for the formation of CNT-walls. Additional, as it is a catalytic process, a catalyst (in this case a metal) is involved to control the kinetics of reactions such as the decomposition of the precursor. Also, it acts as a geometric confinement for the forming the structure of CNT. The catalyst may be located on the substrate or is delivered via the gas phase. Often the latter is termed as a floating catalyst process. On the other hand, for empty CNT apart from the metal-organic compound an additional hydrocarbon (mostly liquid or gaseous) is very often used, the deposition of highly filled carbon nanotubes is realized by only metal-organic compounds. The family of metallocenes (Me-$(C_5H_5)_2$ with Me = transition metals) accommodates both elements (C and Me) in their structure in a fixed ratio of 1:10. Also, as these compounds have a convenient range of temperature for sublimation and thermal decomposition, usually these metallocenes are used precursors for the filled carbon nanotubes synthesis. Especially these metallocenes such as, nickelocene, cobaltocene and ferrocene contain the transition metals Ni , Co and Fe respectively. It is well established that these metals have a relatively low carbon solubility, and form only metastable carbides and thus, are able to act as the efficient catalysts. By using only such metallocenes the filling and the forming of the carbon nanotube is a simultaneous process (the so-called in-situ filling process). The other strategies, such as, for the ex-situ filling of the nanotubes in a separate step after the growth of empty, hollow CNT, filling is carried out.

Various methods for the filling of carbon nanotubes, such as laser ablation, arc-discharge, flame synthesis, electrolysis, high pressure carbon monoxide (HiPco), pyrolysis, ion-beam sputtering, high-temperature heat treatment, and chemical vapor deposition (CVD) have been employed. The arc discharge technique is a popular method, however, a sufficiently high yield for commercial use is difficult to achieve. The CVD method can produce carbon nanotubes and fibers in large quantities. Due to its low cost and simplicity, the technique is perfectly suited for the production of nanomaterials for future industrial applications.

Figure 2.1. Currently used techniques for the sunthesis of CNTs[61]

2.1 Arc Discharge

This is one of the oldest methods of carbon nanotube production. First utilized by Iijima in 1991 at NEC's Fundamental Research Laboratory to produce new type of finite carbon structures consisting of needle-like tubular structures. The tubes were produced using arc discharge evaporation method that is similar to that used for the synthesis of fullerene. In this method, the carbon source with Co, Fe, Ni catalysts located at the discharge region is easily vaporized due to discharge the heat. Vaporization is carried out in a chamber with reduced pressure (~600 mbar), and vapours which include CNTs deposit both on the surface of cathode and on the chamber-wall. These carbon needles, which range in(4 – 30) nm in the diameter and till 1 mm in the length, were grown on negative end of carbon electrode used for the direct current (DC) arc-discharge evaporation of the carbon. During this process, Iijima had used a pressurized chamber which was filled with a gas mixture of 10 Torr of methane and 40 Torr of argon. Two thin electrodes were installed vertically in the center of chamber (as shown in figure below). The lower electrode (cathode) consisted of a small piece of iron in a shallow dip made purposefully

to hold the iron. An arc was generated between the electrodes by running a DC current of 200A at 20V. The use of the three components, namely, methane, argon and iron was critical for the CNT- synthesis. Carbon soot which was produced as result of the arc-discharge settled and nanotubes grew on the iron catalysts contained in negative cathode. The as-produced nanotubes had diameters of about 1 nm with a broad diameter distribution in the range of 0.7 to 1.65 nm.

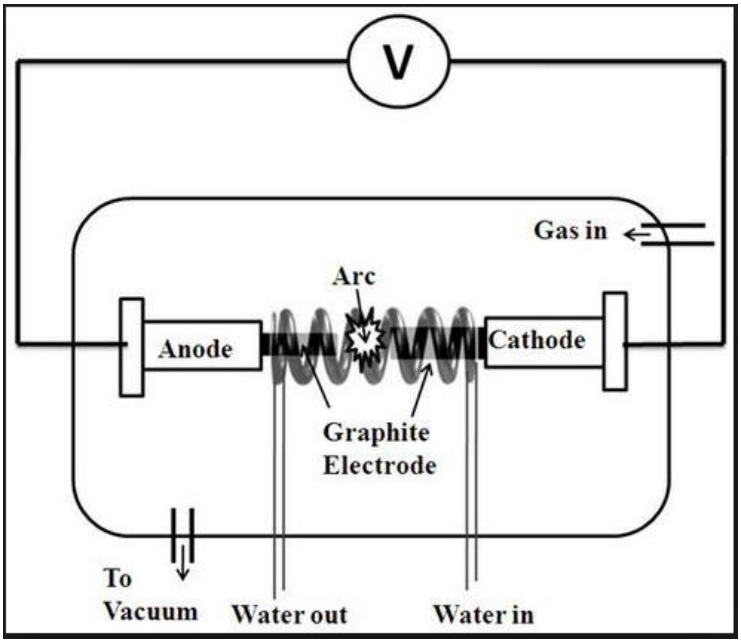

Figure 2-2. Setup for Arc Discharge Method[62]

2.2 Laser Ablation

In the laser ablation process, a strike at graphite target in a high temperature reactor in the presence of inert gas such as helium which vaporizes a graphitic target. As the vaporized carbon condenses, the nanotubes developed on the cooler surfaces of the reactor. Another water-cooled surface is included in the most practical systems to collect the nanotubes (Figure 2). This method was first discovered by Sma -workers in 1995 at Rive University. They were studying the effect of laser impingment on metals at the time of discovery. They produced high yields (>70%) of Single walled Carbon Nanotubes by laser ablation of graphite rods containing small amounts of Ni and Co at 1200˚C. In this method two-step laser ablation was utilized. The initial laser vaporization pulses were followed by the second pulse in order to vaporise target fast. This two step process reduces the carbon-amount deposited as the soot. In this method the tubes grow on

the catalysts atoms and continued to grow until too many atoms aggregate at the end of tube. These tubes synthesized by this method are in the form of mat of ropes 10 - 20 nm in diameter and up to 100 micron or more in the length. By varying the temperature, catalyst composition and also, other process parameters average diameter and length of carbon nanotube could be varied.

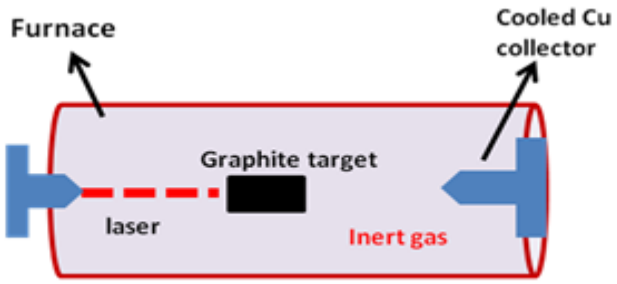

Figure 2-3. Setup of Laser Ablation[63]

2.3 High Pressure Carbon Monoxide Reaction (HiPco)

This is a unique method developed at Rice University in 1999 for the production of carbon nanotubes. Unlike other methods in which the metal catalysts are deposited or embedded on the substrate before the deposition of the carbon initiated, catalyst is introduced in the gas phase in this method. Both the hydrocarbon gas and the catalyst are fed into the furnace, that is followed by catalytic reaction in the gas phase. This method is fit for the large-scale synthesis, as the nanotubes are free from the catalytic supports and thus, the reaction can be operated continuously. CO gas is usually used as the hydrocarbon gas that reacts with iron pentacarbonyl, $Fe(CO)_5$ in order to form SWNT. This process is known as the HiPco process.

In the HiPco process, it is stated that clusters of iron are formed firstly, then nucleation of solid carbon takes place and grows the SWNTs. The iron pentacarbonyl ($Fe(CO)_5$) is injected into stream of CO gas at elevated temperature (800–1,000 °C) and high pressure (≥10 atm). These iron clusters are formed by aggregation of the iron atoms from $Fe(CO)_5$ decomposition at around 250 °C. There are two key functions for iron clusters. They act as the catalysts for the carbon source decomposition and the SWNT formation sites. These clusters grow with additional metal

atoms and the other clusters by collision, eventually reaches a diameter that is comparable to that of SWNT, i.e., 0.7–1.4 nm, which corresponds to 50–200 iron atoms.

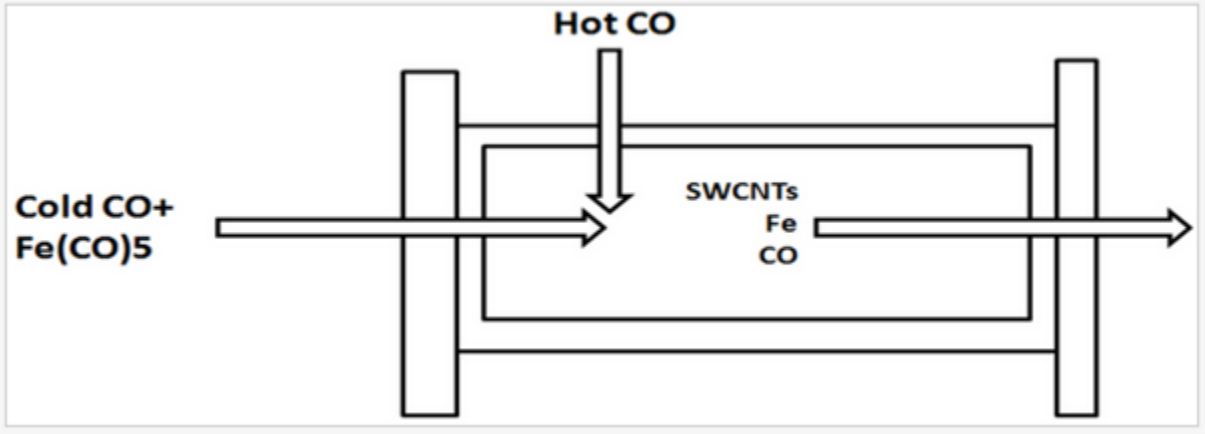

Figure 2-4. Schematic Diagram for HiPco Process[64]

2.4 Chemical Vapour Deposition (CVD)

CVD is a robust method for the growth of high-quality carbon nanotubes that ranges from the single-walled to the multi-walled to the metal-encapsulated carbon nanotubes. This method is fit to produce a large quantity with satisfactory quality and also, allows upscaling at some moderate costs for the industrial mass production. Under the ideal conditions, the CVD growth forms the primarily individual tubes instead of tubes in bundles. Also, the process can be tailored in order to promote either the single- or the multi-walled (MW) carbon nanotubes growth. Amongst the many, thermal CVD was adopted for the experimentation process.

Thermal CVD

There are many different varieties of CVD used to grow CNTs. This is presented pictorially in Figure 2.1. The variations depend on power sources, type of catalyst deposition, gas composition, and operating temperatures. In addition to variations of the CVD process, CNT growth is expected to depend significantly on the chemistry, morphology, and activity of the catalyst and also, the substrate, if involved. In comparison to arc discharge, thermal- CVD

operates at a lower temperature which increases the range of substrate material selections. This method allows the bulk quartz tube surface to act as both the substrate and support for the CNT growth, thus enhancing the contact and adherence of the nanotubes to it and eliminating the requirement of adding an additional substrate in the process.

In the following, the focus is on the in-situ filling processes and the two different methods, which were mainly utilized in experimentation process. Both these processes were carried out under the thermal CVD method. They are illustrated below:

Solid source chemical vapor deposition (SSCVD): For solid source CVD, horizontal quartz tube alongwith a dual zone furnace can be utilized. The general setup for this SSCVD method is illustrated in the figure below. In the initial temperature zone (Tpre << Treac), metallocene powder is placed in quartz boat and is sublimated at a temperature that is compound-specific (e.g., in case of ferrocene, the temperature range is between 100 and 200˚C) directly. This metallocene vapor is then transferred by a controlled nitrogen, argon or hydrogen flow (or a mixture of these gases) into the next (second) temperature zone (Treac) where decomposition of metallocene and the subsequent growth of encapsulated carbon nanotubes takes place. The chosen sublimation temperature (Tpre) strongly determines the rate of sublimation and in association with the rate of argon flow, the amount of metallocene that is transported to the reaction zone. Thus the concentration of metallocene is a function of furnace geometry , temperature, and gas flow. Precursor concentration is the key decisive factor for properties of the as-obtained material. The temperature Treac is preferably changed between 1023 and 1372 K for the deposition of the iron-filled carbon nanotubes. This deposition occurs on certain special substrates located inside hot zone of the reactor alongwith the inner wall of quartz tube reactor. However, the quartz reactor wall is much more provided with the undefined material compared to the aligned as-grown nanotubes on substrate. Generally, silicon substrates with a thin oxide layer are used and an additional coating of these substrates with few nanometer thin metal layer (this metal could be Ni, Fe or Co) lead to much improved deposition behavior as well as higher filling degrees, since these layers act as the secondary catalysts. The simple setup of a typical SSCVD experiment is shown below.

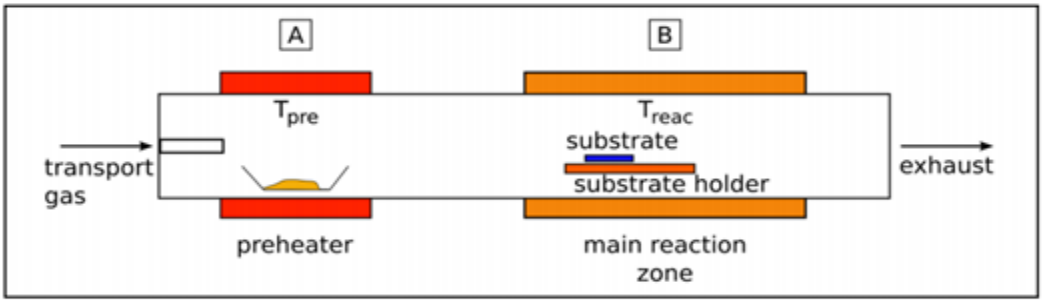

Figure 2.5. Setup of a typical SSCVD experiment. Ferrocene is sublimated in the preheater zone A at temperature Tpre. The decomposition of the precursor and the formation of CNT occurs in the reaction zone B at temperature Treac.[65]

Liquid source chemical vapor deposition (LSCVD): The terminology "liquid source chemical vapor deposition" encompasses all those methods employing solely the liquid precursors as the starting material for the process of deposition. Due to its high adaptability and flexibility, this LSCVD method is broadly used in synthesis of varying unfilled and filled carbon nanotubes. Liquid precursor is either the only source of carbon or it acts as a solvent also for the other precursor compounds. In the case of the carbon nanotube synthesis, liquid precursor is actually a hydrocarbon (heptane,benzene, acetonitrile, etc.) in which metal catalyst compounds (which are in most cases, metallocenes) are dissolved. If these liquids are introduced in CVD reactor, then both the metallocene and the hydrocarbon decompose simultaneously. This is caused by excess high amount of carbon in gaseous phase. Here, predominantly hollow carbon nanotubes with spherical small catalyst particles are formed but no filled CNT are observed with long wires inside their tubes. The experimental design for this LSCVD is simply a dual zone furnace (vertical or horizontal) having an evaporation zone that is followed by the reaction range. The principle setup is illustrated below.

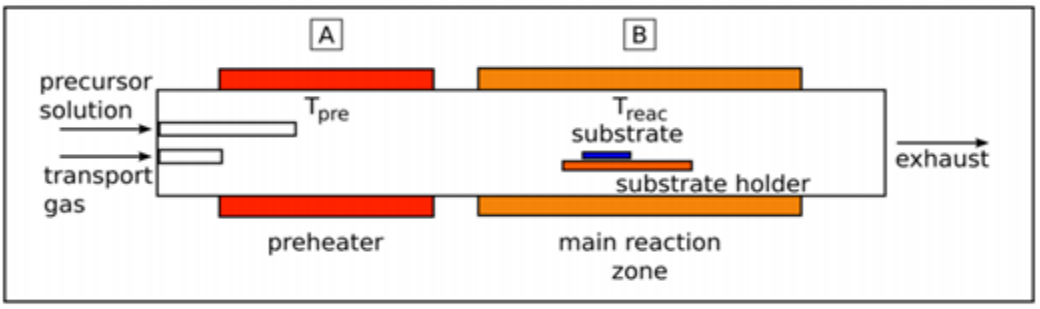

Figure 2.6. Setup of an aerosol experiment. The precursor solution is introduced by a nozzle and diluted by a transport gas flow. The solution evaporates in the preheater zone at temperature Tpre. In the reaction zones both the hydrocarbon and the metallocene decompose at temperature Treac to form the CNT.[66]

Injection of liquid precursor into reactor can be realized in a variety of manners, but mostly, with the aid of an extra inert gas flow like, nitrogen or argon. In reality, in hot zone, decomposition of all the precursor components occurs and thus, the carbon nanotubes are formed. Attraction of this LSCVD method is mainly the ability to precisely control the concentration of used solution (the atom ratio between the carbon and metal component (catalyst) can be accurately regulated in a certain specific range (carbon/metal ratio>> 10).

2.4.1 Discussion of synthesis parameters

Role of the precursor: Choice of the appropriate precursors is crucial for a successful synthesis method for both unfilled and filled carbon nanotubes. The fillings with the ferromagnetic properties at the room temperature are limited to elements like, nickel , iron and cobalt. Organometallic family of the metallocenes, especially nickelocene, ferrocene and cobaltocene consists of these metals in their molecule and thereby they are fit for being precursor for the synthesis of the metal-filled CNT. Besides, their kinetics, their decomposition temperature, and the reactivity of reaction by-products are quite convenient for a successful synthesis method. Another advantage is that these metallocenes can undergo combination. For example, the CNTs with iron or cobalt alloys inside their cavity were obtained by mixing cobaltocene and ferrocene powders or by dissolving both the compounds in the chemical called toluene. These metallocenes are crystalline solid powders at the room temperature. The structure is just like a sandwich with metal in the center and the two cyclopentadiene rings as the ligands. An example is shown in below.

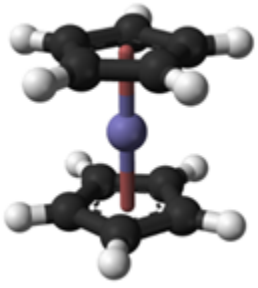

Figure 2.7. Ferrocene molecule[67]

This material can be sublimated in a broad temperature range initiating from 100˚C upto 300˚C. Sublimation behavior specially for ferrocene was extensively studied. For such synthesis, most often a temperature value around 150˚C is inputted as an optimum temperature. Concentration of these metallocene in gas phase at the rated constant transport gas flow can be influenced by setting the sublimation temperature accordingly. The setting of a higher sublimation temperature results in raising the concentration of the metallocene in the gas phase, keeping the transport gas flow at constant rate. An increment of the outer and inner diameters of the iron-encapsulated CNT was seen when ferrocene concentration was elevated. This increment of the outer diameter occurred because more carbon shells were formed by the larger particles. At elevated temperatures, metallocenes would decompose as per the equation below:

$Me(C_5H_5)_2(g) \rightarrow Me(s) + H_2 + CH_4 + C_5H_6 + ...$

whereas moieties depend on the composition of the gas atmosphere and the reaction temperature. Thermal stability of the different metallocenes decrements right from ferrocene over cobaltocene to nickelocene. The ferrocene decomposes above 1073 K but nickelocene decomposes above 550 K already. In contrast, Dyagileva found a pronounced decomposition rate of the ferrocene at 550˚C already in a hydrogen-consisting environment. Because hydrogen is produced during CNT growth, hence, the decomposition starts at around 550˚C and another rise of the reaction temperature would increment the decomposition rate and hence, vary the composition of moieties in gas phase. The metallocenes can be dissolved in liquid hydrocarbons also as applied in LSCVD method mentioned above. Higher the solubility of the ferrocene in the solven, the higher is the probable concentration of the metal in reaction room.

Temperature and Pressure:

Particle size depends on temperature of pretreatment of gas atmosphere and substrate. All reactions in thermal CVD including decomposition, evaporation, and sublimation of the precursors as well as the formation of CNT are ardently temperature dependent. This influence of gas atmosphere and temperature on the CNT- formation are strongly interlinked. The intensive numerical simulation studies have revealed, that reaction temperature affects catalyst particle formation and also the kinetics of gas phase reactions. It was observed that the diameter of the catalyst particles, that are formed spontaneously in gas phase or on the substrate, increments with

the rising temperature. It is confirmed experimentally that the results differ significantly depending on the position of substrate in the reactor. The reasons are in all cases existing temperature profiles in reactor which depend on utilized particular setup. The results confirm that the CNT growth sensitively depends on the gas atmosphere and temperature. Apart from the temperature profiles, every reactor has a set of specific flow conditions which in turn strongly affects the deposition. Due to that, a comparison of experimental results in literature is somewhat difficult.

The most common non-reactive or transport gas is the argon gas. However, nitrogen is also used. Gases which contain Hydrogen such as ammonia (NH_3) or pure hydrogen (H_2) are frequently employed. Since they take part actively in the reaction, they cannot be considered as non-reactive inert gas They are capable of etching away excess carbon from the surface of catalyst particle. This etching of catalyst in order to maintain the activity is a very desired effect. If concentration of the hydrogen is much high then no CNT will be formed but only oil-like deposits will appear. Thus, the growth of CNT will stop at a elevated concentration of the hydrogen. Moreover, this waiver of the unmixed hydrogen may lead to much better growth behavior if argon is only used as the transport gas as Muller could report. Thus, it is assumed that the amount of the H_2 which is produced by ferrocene decomposition is quite sufficient. The entire length of the CNT did not increment with additional H_2 but filling degree did decrease.

From the above discussion, some rules for in-situ filled CNT- formation with different filling degree can be concluded. Firstly, the synthesis of continuous and long filled carbon nanotubes requires to use a precursor with quite low carbon to metal ratio, like, it exists in metallorganic compound family of metallocenes. The metal catalyst layer leads to the higher filling degrees and also a lower diameter distribution of the CNTs, as the secondary source for filling material. For the partially filled CNT, a much higher carbon to metal (catalyst) ratio is needed,as realized by the additional hydrocarbons in precursor. A significantly higher concentration of the active carbon in the relation to metal catalyst woulder lead to less filled CNT. However, since another additional catalyst layer leads to smaller diameter distribution, hence, it is worth consideration.

3. Literature Survey

A literature survey forms an important and indispensable module of a research project. It throws light on the amount of study done so far in the chosen subject matter, showcases the flaws and gaps in the previous research, pinpoints the new scopes of research arising out of those studies, highlights the status of research being carried out by the contemporary research groups in the relevant field around the globe and finally, saves time, funds and energy of a researcher from ending up in some conclusions which have already been found out by some other research group at some early date. Also, it prevents the research knowledge base from being plagued by plagiarism to a great extent.

A substantial amount of literature review has been done in this project. This chapter provides a summary on the different synthesis methods for the growth of filled and unfilled CNTs, adopted by different research groups and their pros and cons as well as their feasibility in commercialization. Moreover, it throws light on the study carried out around the globe on the properties and ways and means to tailor them as per the needs of the semiconductor industry.

Anthuvan Rajesh John et al. [1] synthesized pristine CNTs and nickel-filled CNTs by chemical vapour deposition using lanthanum nickel alloy (LaNi5) particles, both as a catalyst and a source for the Ni-filling. Characterisation techniques such as transmission electron microscopy, X-Ray diffraction and selected area electron diffraction analysis were used for the crystallographic analysis of the encapsulated Ni in the as-produced CNTs. They compared the magnetic properties of the Ni-filled CNTs with that of the pristine CNTs. In addition, they have also suggested the possible growth model involved in the formation of these CNTs.

Uhland Weissker et al.[2] presented an overview about different available chemical vapor deposition (CVD) methods for the synthesis of CNT filled with different ferromagnetic materials such as iron, cobalt or nickel, in addition to the influence of the various growth parameters. Besides that, they evaluated the possible growth mechanisms which are involved in the formation of CNTs. Moreover, they studied their structural and magnetic properties based on which their different application possibilities were presented.

D. Ostling et al.[3] determined the electronic structure of single-wall, multiwall, and filled carbon nanotubes and discuss how their electronic structure evolves from that of single-wall nanotubes. They found that the essential features of the electronic structure in these systems do not depend on the exact atomic positions.

M. Monthioux[4] emphasized on the synthesis of filled CNTs such that the encapsulation of the compound with the surrounding carbon tube allows occurrence of peculiar physical phenomena or peculiar properties can be obtained. A review of the existing literature is carried out extensively, with a focus on C_{60}@SWNTs (peapods), which seems to be the most promising SWNT-based hybrid nano-C_{60} materials till date.

Vıctor M. Garcıa-Suarez et al.[5] simulated a new family of molecular wires based on carbon nanotubes, which can be realized by encapsulating different metallocene molecules in the cavity of the nanotubes. They reported that these wires are resilient to room temperature fluctuations, and expected to have a high yield and also, can be engineered as per design in order to exhibit magnetotransport effects which can be used in spintronics devices.

H.Kataura et al.[6] synthesized four types of single-wall carbon nanotubes (SWNTs) having different diameter distribution and analysed their optical absorption spectra. They compared the three large absorption bands observed due to the optical transitions from infrared to visible region, with the calculated energy band and came up with certain new observations. They found that the absorption Peaks sensitively shifted to the higher energy side with the decreasing tube diameters as predicted by the band calculation. Using the newly found results, they reported that SWNTs can be easily characterized from the optical absorption spectra without transmissd ion electron microscope observations and Raman measurements.

Jianchun Bao et al.[7] fabricated highly-ordered arrays of Ni-encapsulated carbon nanotubes by a second-order template method. This method includes catalytic pyrolysis of acetylene, followed by electrodeposition. They analysed the advantages of this method and stated that this method

should be equally applicable for preparation of different other metal- and alloy-filled carbon nanotubes.

Rajashree Hirlekar et al.[8] reviewed the existing literature on CNTs around the globe. They have summarized the history of Carbon nanotubes (CNTs), right from the chemical composition and physical dimensions to the novel properties that make them potentially way better traditional devices in the relevant fields. The techniques developed for their production of nanotubes in sizeable quantities, are listed by them. The properties and characteristics of CNTs are still to be exploited. They reported that the promising properties of CNTs can bring a revolution in the field of medicines.

M A Zeeshan et al.[9] reported on the growth and the fabrication of Ni-filled multi-walled carbon nanotubes (NiMWNTs) by using template-assisted electrodeposition as well as low pressure chemical vapor deposition (LPCVD) techniques. Anodized templates of alumina oxide (AAO) were fabricated on silicon by using a current controlled method followed by the electrodeposition of Ni nanowires (NWs) by using the galvanostatic pulsed current (PC) electrodeposition method. These Ni NWs served as catalyst in order to grow Ni-MWNTs in an inert atmosphere of H_2/C_2H_2 at an elevated temperature of 700^oC. Characterization was carried out using focused ion beam (FIB) milling, scanning electron microscopy (SEM), transmission electron microscopy (TEM), energy dispersive X-ray spectroscopy (EDX) and Raman spectroscopy. The TEM analysis revealed the fcc structure of the Ni nanowires. vibrating sample magnetometer (VSM) measurements were conducted to understand the effects of electrodeposition parameters, as well as the effects of the elevated temperatures encountered during the MWNT growth upon the magnetic properties of these Ni-MWNTs.

Ferenc Stercel et al.[10] reported the synthesis and the subsequent analysis of metallocenes (such as, chromocene, ferrocene, ruthenocene, tungstenocene-dihydride , vanadocene) encapsulated in the single walled carbon nanotubes (SWNTs). In case of ferrocene, it was observed that efficient filling of SWNTs was carried out from both liquid and vapor phase. The other two metallocenes were encapsulated only from the vapor phase. The high resolution transmission electron microscopy shows single molecular chains of these metallocenes inside the SWNTs. The

molecules are found to move under the beam of electrons in the SWNTs which indicates the absence of strong chemical bonds amongst them and wall of SWNT. However, their movement is found to freeze after a short illumination because of irradiation damage. The energy dispersive X-ray spectrometry is reported to have confirmed the presence of chromium, iron, ruthenium, tungsten, and vanadium.

Uhland Weissker et al.[11] gave an overview about the different chemical vapor deposition (CVD) methods for the synthesis of ferromagnetic metal encapsulated carbon nanotubes and discuss the influence of the selected growth parameters. Moreover, they evaluated possible growth mechanisms that involved in the formation of these filled CNTs and observed their identified magnetic and structural properties. Based on these properties, they presented different application possibilities, including the field of medicine and nanotechnology.

G. Che et al.[12] have developed a novel approach for the preparation of graphitic carbon nanotube and nanofiber ensembles. This approach comprises of chemical vapor deposition (CVD) based synthesis of carbon inside the pores of an alumina based template membrane with or without Ni catalyst. Pyrene or ethylene was used in this CVD process with furnace temperatures of about 545 °C for Ni-catalyzed CVD while 900 °C for the uncatalyzed one. The as-synthesized carbon nanostructures were uniform hollow tubes having open ends. On increasing the deposition time the carbon nanotubes gets converted into carbon nanofibers. Electron diffraction data and transmission electron microscopy show the as-deposited graphitic carbon nanofibers that were synthesized with Ni catalyst were found to be not highly ordered. However, heating these carbon-containing membranes at 500 °C for 36 h, converts these carbon nanofibers into highly ordered graphite.

A. Leonhardt et al.[13] described the synthesis of Fe-, Ni- and Co-encapsulated carbon nanotubes with the aid of the chemical vapor deposition method. They have obtained filled nanotubes with different thicknesses of the carbon walls and relatively uniform core diameters, by varying the deposition conditions. The filled carbon nanotubes are characterised by energy dispersive X-ray analysis and transmission and scanning electron microscopy. The magnetic behaviour of the aligned Fe-filled tubes was analysed by using alternating electron holography and gradient

magnetometry measurements. The observed enhanced coercivities are significantly higher than in bulk Fe.

Pawan K. Tyagi et al.[14] reported that Carbon nanotubes (CNTs) encapsulated with ferromagnetic materials have the potentials for use in the magnetic scanning probe microscopy and also, as an assembly of high density aligned magnetic nanocores for the future magnetic data storage devices. These uniform and highly ordered Ni-filled CNTs were deposited by chemical vapour deposition and were characterized using transmission Raman spectroscopy , nano-area diffraction and electron microscopy. The magnetic properties of Ni-filled CNTs were investigated using superconducting quantum interference device analysis showed better ferromagnetism compared to the bulk Ni.

4. Experimental Procedure

In this chapter we will discuss all the experiments carried out throughout the span of project work, their set ups, yield, methodology and how we came up with the optimized procedure. All the experimental work was carried out in the Nano fabrication lab, Department of Applied physics at DTU.

4.1 Synthesis technique adopted: Thermal CVD

Thermal CVD is a robust method for the growth of high-quality carbon nanotubes that ranges from the single-walled to the multi-walled to the metal-encapsulated carbon nanotubes. This method is fit to produce a large quantity with satisfactory quality and also, allows upscaling at some moderate costs for the industrial mass production. Under the ideal conditions, thermal CVD growth forms the primarily individual tubes instead of tubes in bundles. Also, the process can be tailored in order to promote either the single- or the multi-walled (MW) carbon nanotubes growth. This in situ filling of CNTs using thermal CVD with nickel finds application in the magnetic scanning probe microscopy as well as the assembly of aligned high density magnetic nanocores for future magnetic data storage devices. A real time lab set up for Thermal CVD is given below.

Figure 4.1. Picture of CVD furnace @DTU

4.2 Required Apparatus and Precursors used

In order to complete the entire set up of experiment a number of apparatus and precursors are needed, here in this topic we will name and if necessary, explain each one of them.

1. **Silicone pipe**: To tranport the precursors inside the tube to carry out the reactions it is needed. The length of used pipe in our experiment is 1 m with an internal diameter of 38 mm and external diameter of 40 mm.
2. **Ultrasonicator**: As in this experiment a solution of metallocene with the hydrocarbon is required so to make such solution ultrasonication is performed.
3. **Thermal CVD furnace**: This requirement is shown in the above section.
4. **Quartz tube**: This tube goes inside the furnace and in the hot zone of this tube the reactions are carried out.
5. **Hydrogen and Argon gas cylinders**
6. **Gas Flow meter**
7. **Nickelocene**: It provides for the encapsulated Ni inside the synthesized CNTs.
8. **Benzene**: It has a two-fold role in the experimental process – firstly, being the provider of carbon for CNT preparation and secondly, as a solvent for Nickelocene.

4.3 Optimization of Synthesis Parameters

The entire experiment is optimized in order to get better yield according to three parameters namely, temperature, concentration of Nickelocene and gas flow.

1. **Temperature**: The synthesis of Ni filled CNTs are carried out on various temperature as the production of CNTs starts at 600 °C but the yield is very low so in order to get a better yield the temperature of the furnace is varied and in the beginning of the experiments it was kept around 850 °C which then reduced to 820 °C in order to get a better yield.

2. **Concentration of Nickelocene**: It is very crucial to keep an adequate amount of Nickelocene as it provides for the encapsulated metal amd if kept low only hollow CNTs are going to be synthesized. And if kept high encapsulation might not even take place.
3. **Gas flow rate**: It is another very important factor which plays a crucial role in the formation of filled CNTs and during the course of our experiment it has been varied to get the best possible result.

4.4 Experimental work

Upon going through a lot of literatures i decided to start the work but until now I was not decided upon the solvent because there were a number of non polar solvents like Toulene, Benzene, Di chlorobenzene, THF etc. but solubility of nickelocene was still a concern and in order to make a solution, I decided to sonicate the solvent(Benzene)and the solute(Nickelocene).

Any Non polar solvent will solve the purpose but I decided to use Benzene because of its ready availability and less toxicity in comparison to Xylene.

Steps in experiment:

1. Cleaning of quartz tube.
2. Making the solution of Nickelocene and Benzene.
3. Setting up the furnace with protection and precaution.
4. Obtaining the synthesized sample.
5. Removal of Non magnetic impurity from sample.

4.4.1 Flow chart

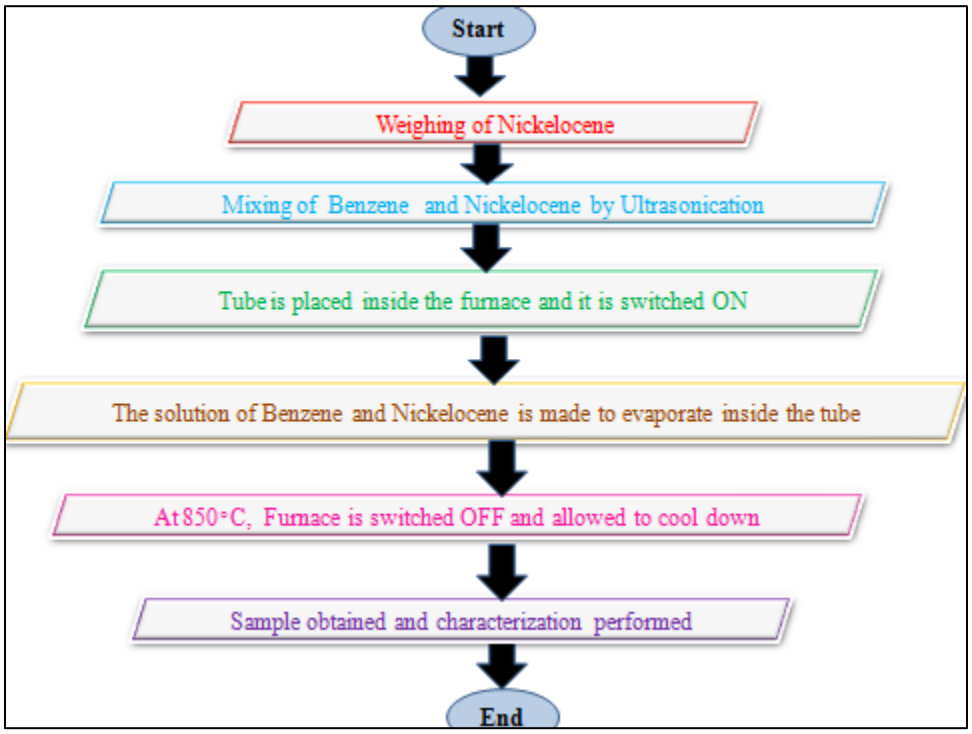

Figure 4.2. Flow Chart of the entire experimental process

4.4.2 Flow Diagram

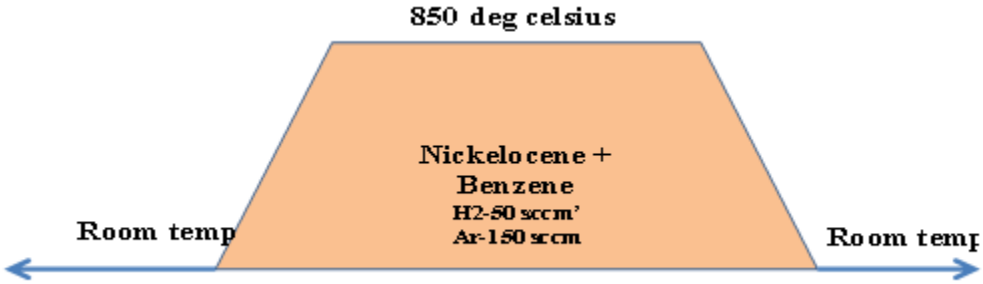

Figure 4.3. Flow Diagram of the entire experimental process

The above diagram is an approximate flow for the entire furnace process. Here, it is simply a generic one in order to understand the technique but later in our experimental trials, we will see that process might be altered in order to optimize the yield.

Here it is being shown that the entire process will start at a room temperature and goes linearly up to a desired temperature (850 °C in this case) with the solution of the precursors inside the tube as well as with required gas flow of hydrogen and argon. Some what this is the process which I followed throughout all the experiment barring a few. Now I will give the experimental details one by one for every experiment.

4.4.3 Pictorial representation of experiment

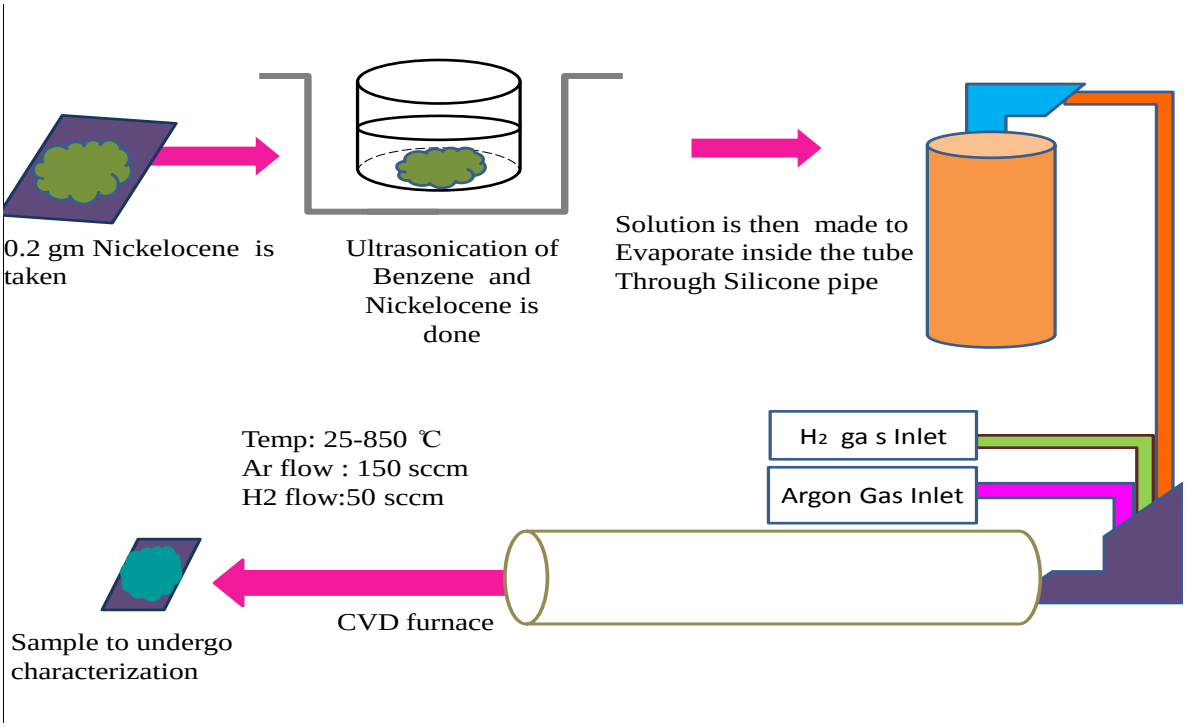

Figure 4.4. Block Diagram of the entire Experimental Process

4.4.4 Schematic Diagram

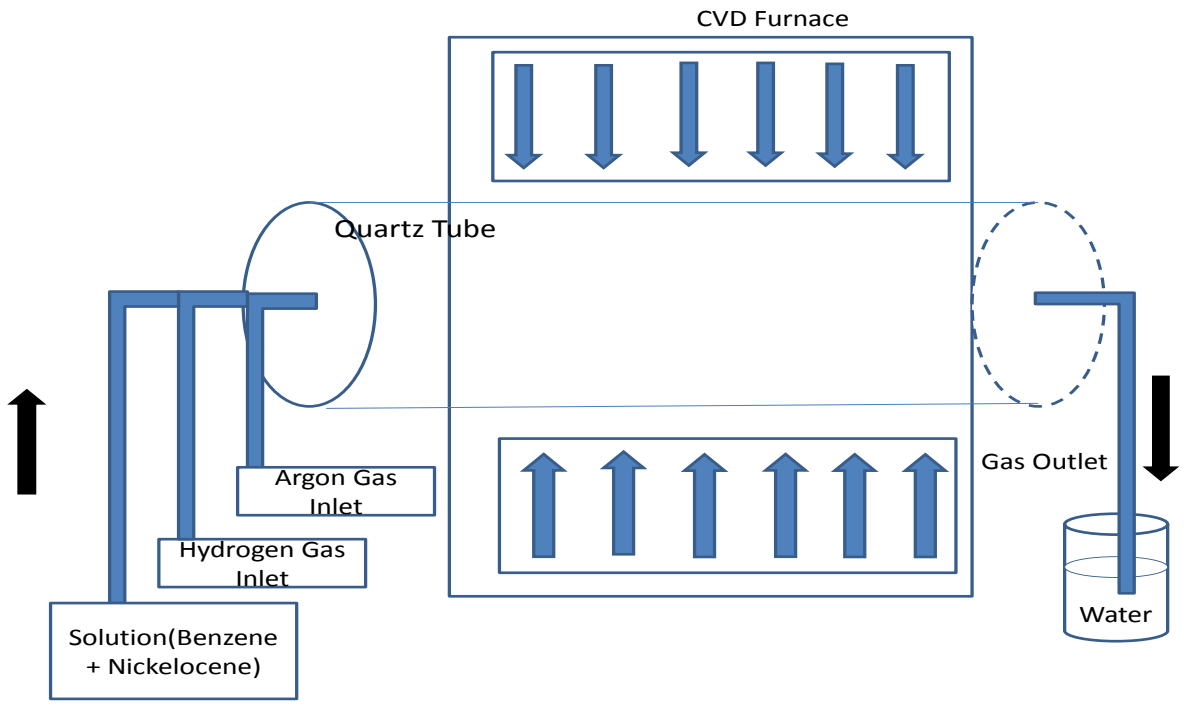

Figure 4.5. Schematic diagram of CVD furnace

Trial no. 1

a. Cleaning of quartz tube

The quartz tube is a cylindrical tube which has heat handling capacity better than glass and as the technique used here is Thermal CVD, it is bound to be in the range of 500 to 1000 °C. The tube is being cleaned using hydrochloric acid with a concentrated measure so proper precaution like rubber shoes, gloves, apron should be taken and wore. I cleaned the tube thoroughly twice and let it dry and again the next day it has been cleaned with the use of Acetone for left over impurities and again left to evaporate.

b. Making the solution of Nickelocene and Benzene.

The solution is made by the use of ultrasonication process where the solute and the solvent are kept in the sonicator and shaked at a very high frequency in order to mix them

properly. Sonication is a method in which sound waves are used to agitate particles in the solution. Such disturbances can be used to mix solutions, speed the dissolution of a solid into a liquid (like sugar into water), and can remove dissolved gas from liquids in some cases too.

In the very first trial I took 20 ml of Benzene and mixed 0.2 gm of Nickelocene in it and sonicated it for 10 min, the obtained solution was a not a true solution but there were no suspension visible to naked eye as well as there were no sedimentation. Once the solution was prepared it as kept in the bottle with the nozzle and e start preparing the furnace.

c. Setting up the furnace

The thermal CVD furnace in the laboratory is checked and the quartz tube is inserted into it, on the one side the quartz tube is attached with the silicone pipe to the bottle containing solution and to the gas cylinder through gas regulator which regulates the flow rate as well as displays the rate.

The other side of the tube is connected to the thermocouple for getting time to time exact temperature of the tube's inside and also this side is being used to release the waste fume out of the tube. Once the furnace set up is done we start the furnace with room temperature take it up to 850 °C and once this temperature is reached the solution is made to evaporate inside the tube and once all the solution is evaporated we started cooling down the furnace back to room temperature.

d. Collection of sample

The next day of the experiment the cooled quartz tube is taken out of the furnace and the deposited black powder/ flake on the wall of the tube is scratched with the help of a brush and a rod. The obtained sample is carefully taken into a vial and kept for characterization.

e. Removal of non magnetic impurities

A simple technique is used to remove non magnetic that is un-encapsulated carbon nanotube from the sample. A magnet is used to attract the encapsulated carbon nanotubes and only that is kept as a sample and rest is thrown in the trash. Thus obtained sample is sent for characterization.

Figure 4.6. Removal of non magnetic elements from the as-obtained sample

Amount of precursor	Gas used	Flow rate	Temperature	Sonication
20 ml Benzene 0.2gm Nickelocene	Hydrogen Argon	50 sccm 150 sccm	25 to 850 °C	10 min

Table 1. Specifications relating to Trial no.1

Trial no. 2

Due to the poor yield and non uniformity in the first time, we changed the amount of Benzene used and instead of taking 20 ml we took 10 ml of Benzene and kept all other conditions same.

Amount of precursor	Gas used	Flow rate	Temperature	Sonication
10 ml Benzene 0.2 gm Nickelocene	Hydrogen Argon	50 sccm 150 sccm	25 to 850 °C	10 min

Table 2. Specifications relating to Trial no.2

Trial no. 3

Although the sample prepared was uniform but in order to get a optimized experimental condition we keep on changing the parameters so this time around no sonication is done.

Amount of precursor	Gas used	Flow rate	Temperature	Sonication
10 ml Benzene 0.2gm Nickelocene	Hydrogen Argon	50 sccm 150 sccm	25 to 850 °C	NIL

Table 3. Specifications relating to Trial no.3

Trial no. 4

As sometimes only hydrogen gas is able to carry out the reactions in the case of synthesis of carbon nanotube. So I thought of doing the same for synthesis of filled nanotube, but the attempt went in vain as negligible or no CNTs preparation took place.

Amount of precursor	Gas used	Flow rate	Temperature	Sonication
10 ml Benzene 0.2 gm Nickelocene	Hydrogen	50 sccm	25 to 850 °C	10 Min

Table 4. Specifications relating to Trial no.4

4.5 Intermediate work

After the first trial consisting of four runs with satisfying result in couple of them, I changed the procedure a little bit in order to land up with the final and optimized conditions.

4.5.1 Flow Diagram

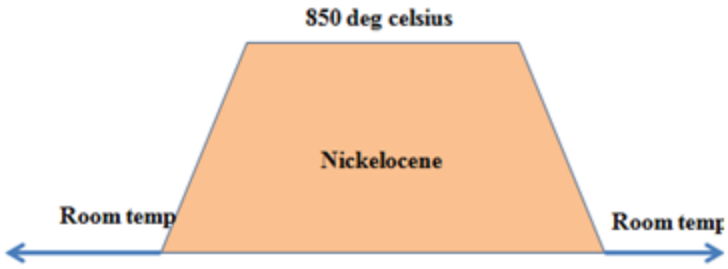

Figure 4.7. Flow Diagram of the experimental Procedure

The above diagram is an approximate flow for the entire furnace process. Here it is simply a generic one in order to understand the technique but later in our experimental trials we will see that process might be altered in order to optimize the yield.

Here it is being shown that the entire process will start at a room temperature and goes linearly up to a desired temperature(850 °C in this case) with the powder of Nickelocene on to a boat inside the tube as well as with required gas flow of hydrogen and argon. Some what this is the process which I followed throughout all the experiment barring a few. Now I will give the experimental details one by one for every experiment.

4.5.2 Schematic Diagram

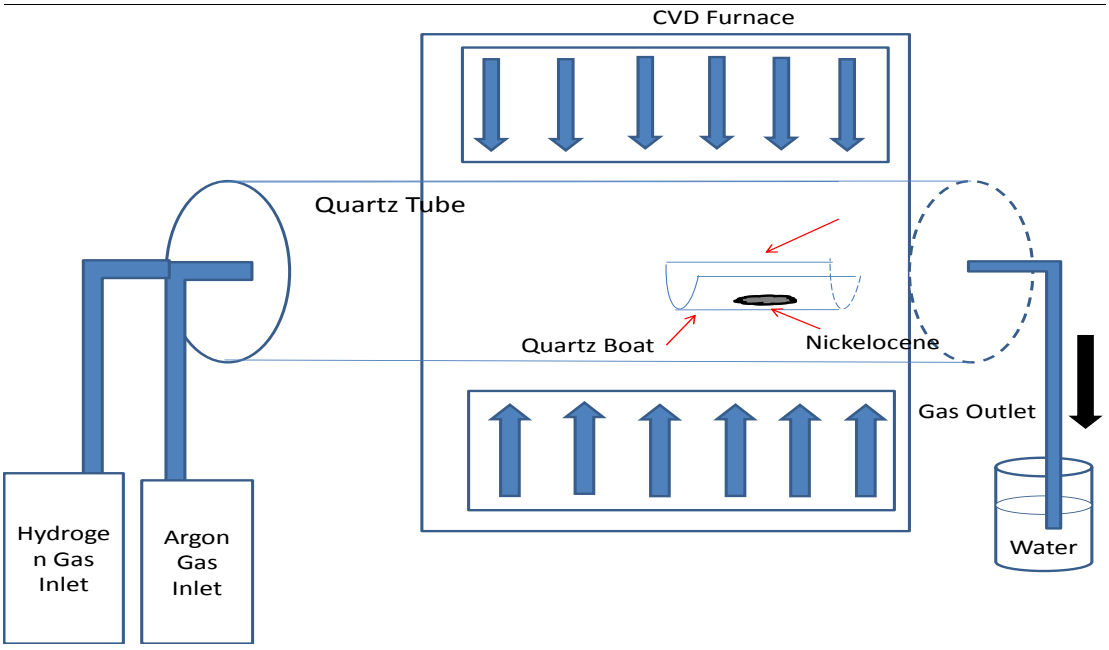

Figure 4.8. Schematic of CVD set up

Trial no. 5

During my intermediate work instead of making a solution of Nickelocene and Benzene I tried pyrolysis where the main precursor Nickelocene is kept on a quartz boat into the tube and once the desired temperature is reached the reactions takes place and filled CNTs are formed.

Amount of precursor	Gas used	Flow rate	Temperature
0.2 gm Nickelocene	Hydrogen Argon	50 sccm 150 sccm	25 to 850 °C

Table 5. Specifications relating to Trial no.5

In this trial too sample is formed but I was not able to better the yield as seen from the SEM results so this method was written off and the previous methodology is considered the best one and tried emulating it further in upcoming Successful and Optimized work.

4.6 Successful and Optimized Work

In order to get the best result Trial no. 2 was repeated with a minor change of temperature (here taken 820 °C instead of 850 °C), the uniformity of the sample was there in that case as well as there were certain other characterized result like XRD which supported the theory so now I went for some more characterization techniques like TEM and RAMAN SPECTROSCOPY which results were also in accord with the standard one. So now the challenge was to repeat it twice in order to prove it was reproducible.

Trial no.6

4.6.1 Flow diagram

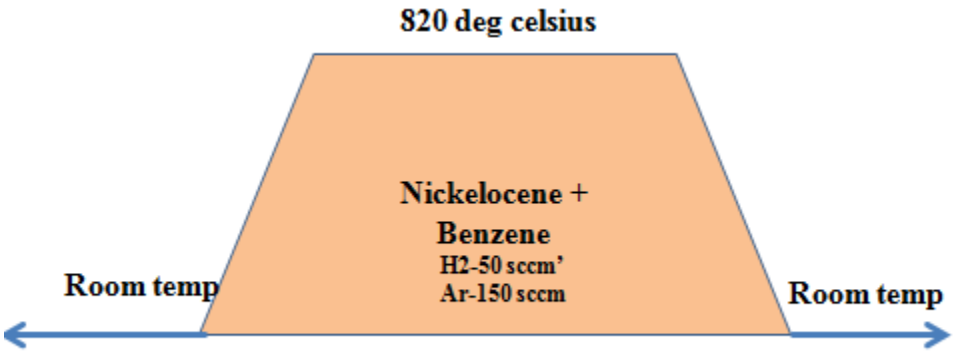

Figure 4.9. Flow Diagram of the Experimental Procedure

We started with the room temperature and went upto 850 °C and then the solution was made to evaporate inside the tube.

4.6.2 Schematic Diagram

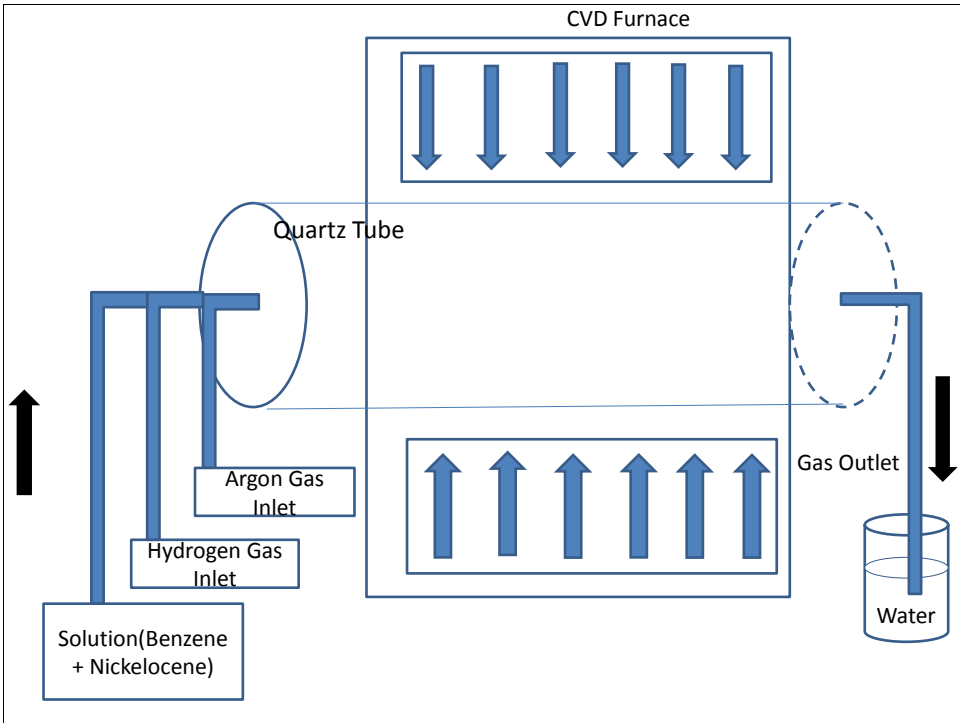

Figure 4.10. Schematic of CVD set up

Optimized Condition

Amount of precursor	Gas used	Flow rate	Temperature	Sonication
20 ml Benzene 0.2 gm Nickelocene	Hydrogen Argon	50 sccm 150 sccm	25 to 820 °C	10 min

Table 6. Specifications relating to Trial no.6

The above set of parameters were kept the same for the next the trials, 7 and 8 and the results obtained were just like the trial no. 6. Hence, concluding the fact that it can be repeated.

5. Methods of Characterization

Characterization techniques are referred to those methods through which one can identify an as-prepared sample with respect to its morphology, surface topology, internal structure, composition, etc. The characterization techniques used to study a sample, depends on its properties, features, tolerance to the imposed environment so that during the process, no damage is done to the sample either internally or externally.

In order to analyse the as-grown CNTs samples, a few tools capable of characterising them at a microscopic and below scale were necessary as the crystal compound growths were expected to be up to several nanometres in size. On account of the focus upon streamlining the growth process and thereby, obtaining single dimension growths, the following powerful techniques of characterizing the samples were necessitated. The set up and working of these techniques are briefly summarized below:

5.1 X-Ray Diffraction (XRD)

It uses the spatial distribution and intensities of X-ray radiation scattered by the sample under study and helps in the investigation of the structure of the sample. X-ray diffraction analysis technique has been used successfully to establish the atomic crystalline samples because crystals have a rigid periodicity in structure and constitutes naturally produced diffraction gratings for X rays. When X radiation interacts with the electrons of a sample, the X rays are diffracted accordingly. The pattern of the diffraction depends on the wavelength of the X rays employed and on the structure of the object.

Crystals can be understood as regular arrays of atoms, and X-rays are considered as waves of electromagnetic radiation. Atoms scatter X-ray waves, mostly through the atoms' electrons. Just as an sea wave striking a beach lighthouse produces secondary circular waves emerging from the lighthouse, so an X-ray striking the electron produces secondary spherical waves emerging from the electron. This phenomenon is called as elastic scattering, and the electron (or lighthouse) is called as the *scatterer*. A regular array of such scatterers produces a regular array of spherical in nature waves. Even though these waves cancel one another out in most of the directions

through destructive interference, they might add constructively in a few specific directions, and that is determined by Bragg's law. X-ray scattering is a kind of elastic scattering; so the outgoing X-rays have the same energy, and hence the same wavelength, as the incoming X-rays, only with changed direction. These specific directions can be seen as spots on the diffraction pattern called *reflections*. Hence, X-ray diffraction results from an electromagnetic wave (the X-ray) impinging on a regular array of scatterers (the repeated arrangement of atoms within the crystal).

X-rays are commonly used to produce the diffraction pattern and the reason is their wavelength λ which is typically the same order of magnitude (1–100 angstroms) as that of spacing *d* between planes in the sample's crystal.

As the wavelength of x-ray is in the range with the lattice parameter of the crystals, diffractions might be happening when it interact with the sample's surface. According to the Bragg law, diffraction happens only if the stated condition is verified

$$2d\sin\theta = n\lambda$$

With particular incoming x-ray wavelength (λ), the diffraction angle (θ) is related to the planar distance of crystals (d), as shown in the figure below. Thus from the diffraction spectrum, the information crystal structure can be produced. One of the biggest advantage of XRD is that it is a non-destructive analytical method which can be used to identify phase as well as orientation, to determine structural properties, to measure the thickness of thin films, estimate the size of nanoparticles, etc.

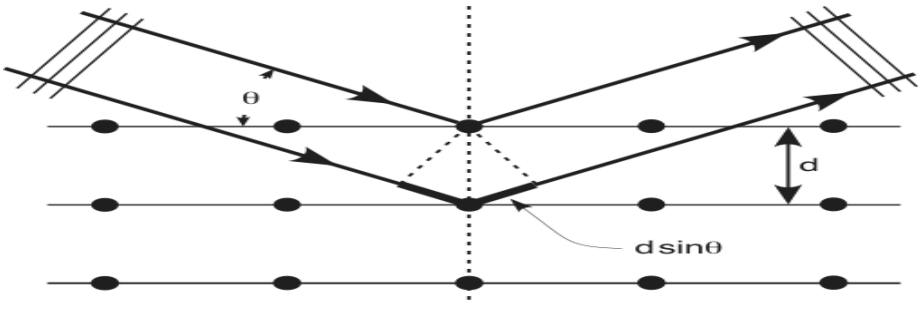

Fig. 5.1. Bragg diffraction[68]

Figure 5.2. Picture of XRD set up @DTU

5.2 Scanning Electron Microscopy (SEM)

It is a type of electron microscope that creates images of a sample by scanning the sample with a focused beam of electrons. The electrons interact with the sample's atom, producing many types of signals that can be detected and that contain information about the sample's surface topography and composition. The electron beam is usually scanned in a raster scan pattern, and the position of the beam is combined with the detected signal to produce an image. SEM can achieve a very high resolution, even finer than 1 nanometer.

The most used SEM mode is the detection of secondary electrons emitted by atoms which are excited by the electron beam. The amount of secondary electrons depends on the angle at which beam meets specimen surface, i.e. on specimen topography. By scanning the sample and by collecting the secondary electrons with the use of a special kind of detector, an image displaying

the topographical information of the surface is formed, revealing minute details less than 1 nanometer in size.

SEM is typically consisted of the following features:

- A source (electron gun) of the electron beam which is accelerated down the column.
- A series of lenses(objective and condenser) which act to control the diameter of the beam as well as to focus the beam on the specimen
- A series of apertures (micro scale holes in metal films) through which the beam passes and which affects properties of that beam
- Controls for specimen position (x,y,z-height) as well as orientation (tilt, rotation);
- An area of beam/interaction which generates several types of signals that can be detected and processed so as to produce an image or spectra; and
- All the above components are maintained at high vacuum levels.

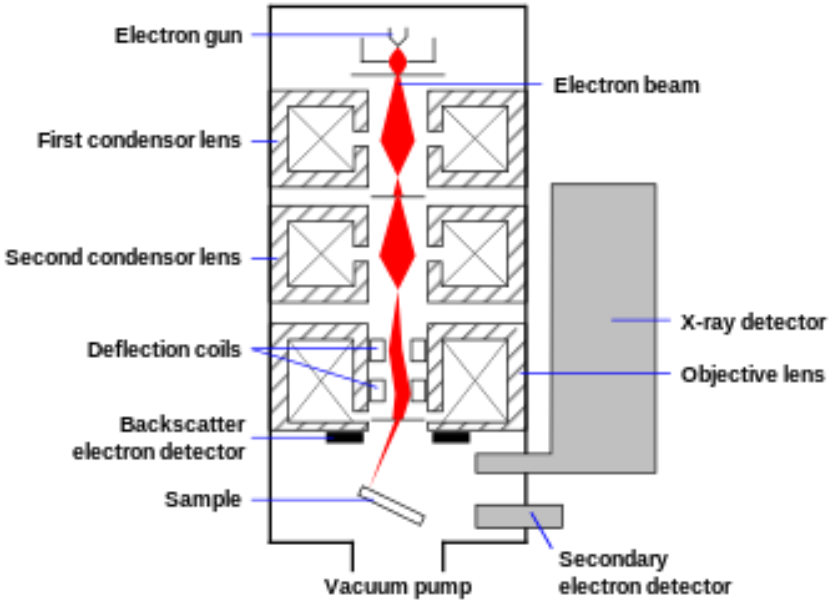

Figure 5.3. Schematic of SEM apparatus[69]

Figure 5.4. Picture of SEM set up @DTU

Typically, in a SEM, an electron beam is thermionic in nature which is emitted from an electron gun that is equipped with a tungsten filament cathode. The electron beam, which has an energy generally ranging from 0.2 keV to 40 keV, is focused by one or may be two condenser lenses to a spot that is about 0.4 nm to 5 nm in diameter. The beam then passes through couple of scanning coils or pairs of deflector plate present in electron column, generally in the final lens, which then deflects the beam in the *x* and *y* axes in such a way that it scans in a raster fashion to cover a rectangular area of the sample's surface. The beam is rastered starting from left to right and from top to bottom. There is a direct one-to-one correspondence between the rastering pattern of the specimen and the rastering pattern that is being used to produce the image on monitor. The resolution chosen to image affects the number of pixels in each row as well as the total number of rows of the the scanned area. When primary beam of electrons interacts with the sample, the electrons loses their energy by repeated random absorption and scattering within the

interaction volume, which is normally less than 100 nm to approximately 5 µm into the surface. The types of signals produced by a SEM include back-scattered electrons (BSE), secondary electrons (SE), characteristic X-rays ,Auger electrons, light (cathodoluminescence) (CL).

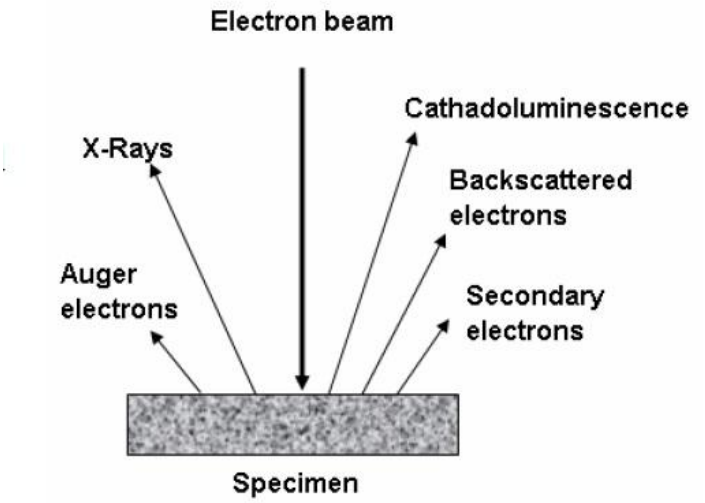

Figure 5.5. Different types of electrons released during SEM imaging[70]

1) Secondary Electrons: If an incident electron collides with an electron in a sample atom, it will knock that electron out of its orbital shell and the atom becomes ionized. Because the incident electron loses only a little energy during each collision, hence, multiple collisions are possible, continuing until the incident electron has no more energy to dislodge secondary electrons. Each freed secondary electron has a small kinetic energy (<50 eV), and this energy is independent of the energy of the incident electron. If generated close enough to the sample surface (<10 nm), these secondary electrons can escape from the sample and can be collected by the detector. As a result, secondary electron imaging is closely related to sample topography.

2) Backscattered Electrons: If an incident electron collides with the nucleus of a surface atom, then the electron will bounce back or scatter 'backward' out of the sample as a backscattered electron (BSE). These electrons have high energies, typically in the range of 50 eV and that of the original incident electron. The production of these BSE electrons varies directly with atomic number, and thus backscattered electron images can be used in order to discern differences in sample atomic number.

3) Auger Electrons: As a result of generation of secondary electron, a vacancy is left in an ionized atom's electron shell. In order to fill this vacancy, an electron from a higher energy outer shell (from the same atom) can drop down to fill the vacancy. This creates a surplus energy in the atom that can be corrected by emitting an outer electron, which is an Auger electron. Auger electrons have a characteristic energy unique to the element from which they are emitted and hence, can be used to give compositional information about the target sample. However, Auger electrons have a relatively low kinetic energy and are only emitted from shallow sample depths (<3 nm).

4) Characteristic X-rays: X-rays are also produced due to interactions of the incident electron beam with the sample's surface. Just like the Auger electron generating process, the excess energy produced as a result of reshuffling electrons to fill shell vacancies can also be emitted in the form of an X-ray rather than an Auger electron. X-rays have a characteristic energy unique to the element from which they are emitted and so provide compositional information about the sample.

5.3 Raman Spectroscopy

This spectroscopic technique is generally used to observe vibrational, rotational, and some other low-frequency modes in a given system. Raman spectroscopy is usually used in chemistry to provide a fingerprint by which different molecules can be identified. It is a spectroscopic technique based on the inelastic scattering of monochromatic light unlike XRD, usually from a laser source. Here inelastic scattering means that the frequency of photons in monochromatic light changes upon interaction with the sample. Photons of the laser light are absorbed by the sample and then emitted. The frequency of the reemitted photons has a shift either in up or down direction when compared to the original monochromatic frequency, which is known as the Raman effect. This shift is capable of providing information about vibrational, rotational as well as other low frequency transitions in molecules.

The Raman effect occurs due to inelastic scattering of photons by matter which may be solid, liquid or gas. This effect is observed as a shift in the frequency of the scattered light relative to the excitation frequency. These energy transitions are due to molecular vibrations. Because these

vibrations consists identifiable functional groups, when energies of these transitions are plotted as in a spectrum, they can be used to identify the molecule.

A Raman system typically consists of four major components:

1. Excitation source (Laser).
2. Sample illumination system and light collection optics.
3. Wavelength selector (Filter or Spectrophotometer).
4. Detector (Photodiode array, PMT or CCD).

Typically, a sample is illuminated with the help of a laser beam. Electromagnetic radiations from the illuminated spot is collected with a lens and then sent through a monochromator. Elastic scattered radiation at wavelength corresponding to that of laser line (Rayleigh scattering) is filtered out, however the rest of the collected light is dispersed onto a detector by a notch filter or a band pass filter.

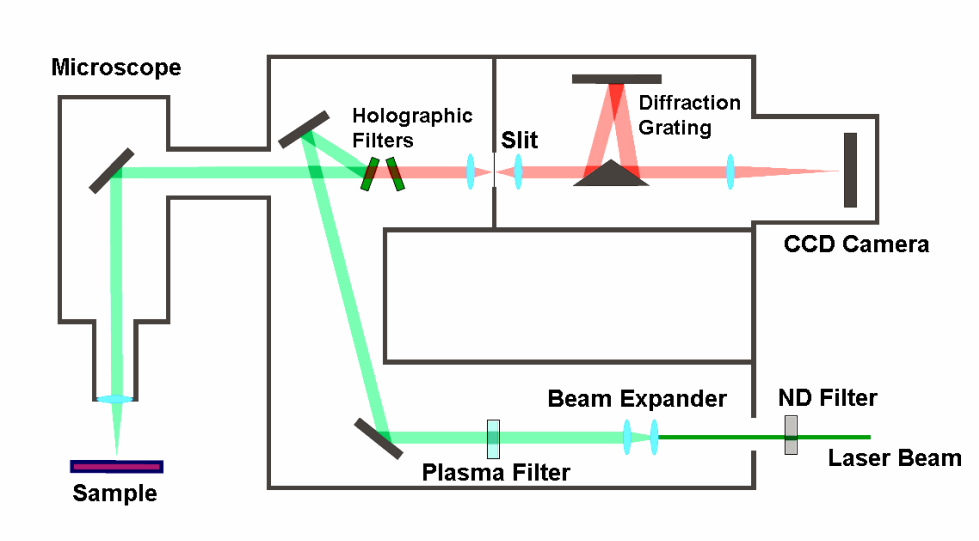

Figure 5.6. Schematic diagram of a Raman spectrometer.[71]

Raman shifts are generally reported in wavenumbers, having units of inverse length, as this value is directly related to energy. In order to convert between spectral wavelength and wavenumbers of shift in the Raman spectrum, the following formula is used:

$$\Delta w = \left(\frac{1}{\lambda_0} - \frac{1}{\lambda_1}\right) ,$$

where Δw is the Raman shift expressed in wavenumber

λ_0 is the excitation wavelength

and λ_1 is the Raman spectrum wavelength.

The main advantages of Raman spectroscopy are its lack of sample preparation, high information content compatibility with aqueous systems, and non-destructive nature.

5.6 Transmission Electron Microscopy (TEM)

It is a microscopy technique in which the beam of electrons is made to transmitt through an very thin specimen, interacting with the specimen as it passes through it. An image is then formed by the interaction of the electrons which transmitted through the specimen, then the image is magnified and focused onto an imaging device, like a fluorescent screen, or on a layer of photographic film, or it can be detected by the use of a sensor. TEMs are capable of imaging at a much higher resolution than optical microscopes, due to the small de Broglie wavelength of the electrons. At smaller magnifications TEM image contrast is because of absorption of electrons in the material, or due to the thickness and composition of the material. At much higher magnifications complex wave interactions modulate the intensity of the produced image, requiring professional analysis of observed images. Alternate modes of use allow the TEM to observe modulations in crystal orientation, electronic structure, chemical identity and sample induced electron phase shift and the regular absorption based imaging. TEM forms a important analysis methodology in a range of scientific fields, in both physical as well as biological sciences.

Transmission electron microscopy (TEM) uses very high energy electrons to penetrate through an ultrathin (≤100 nm) sample. This can increase spatial resolution in imaging (down to individual atoms) and the possibility of carrying out diffraction from nano-sized volumes. When electrons are accelerated up to a high energy levels (few hundreds keV) and focused onto a material, they can scatter or might backscatter elastically or inelastically, or even produce many

interactions, source of different signals such as X-rays, Auger electrons or light. Some of them can be used in transmission electron microscopy (TEM).

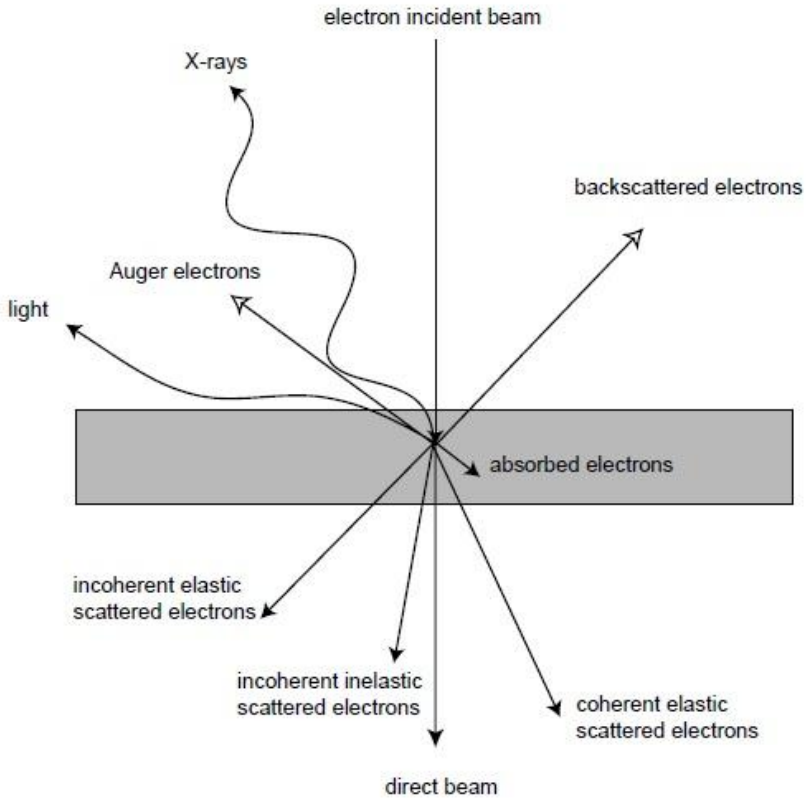

Figure 5.7. Different types of signals produced during TEM imaging[72]

Like all other matter, electrons have both wave as well as particle properties (as theorized by Louis-Victor de Broglie), and their wave like properties means that a beam of electrons can behave like a beam of electromagnetic radiation. The wavelength of electrons is directly related to their kinetic energy via the de Broglie equation. An additional correction must be made here to account for relativistic effects, as in a TEM an electron's velocity reaches very close to the speed of light, *c*.

$$\lambda_e \approx \frac{h}{\sqrt{2m_0E\left(1+\frac{E}{2m_0c^2}\right)}}$$

where, h is Planck's constant, E is the energy of the accelerated electron and m_0 is the rest mass of an electron. Electrons are generally generated in an electron microscope by a particular process known as thermionic emission from a filament, commonly tungsten, in the same manner as that of a light bulb, or by field electron emission. The electrons are then accelerated using an electric voltage and focused by electrostatic as well as by electromagnetic lenses to the sample. The transmitted beam consists information about phase, electron density and periodicity; this beam is used to form the image.

TEM operates mainly in two modes, namely,

(A) Imaging Mode

(B) Diffraction Mode

A transmission electron microscope is made up of:

(1) Two or three condenser lenses to focus the electron beam onto the sample,

(2) An objective lens in order to form the diffraction in the back focal plane and the image of the sample on the image plane,

(3) Some intermediate lenses to magnify the image or the diffraction pattern on the screen.

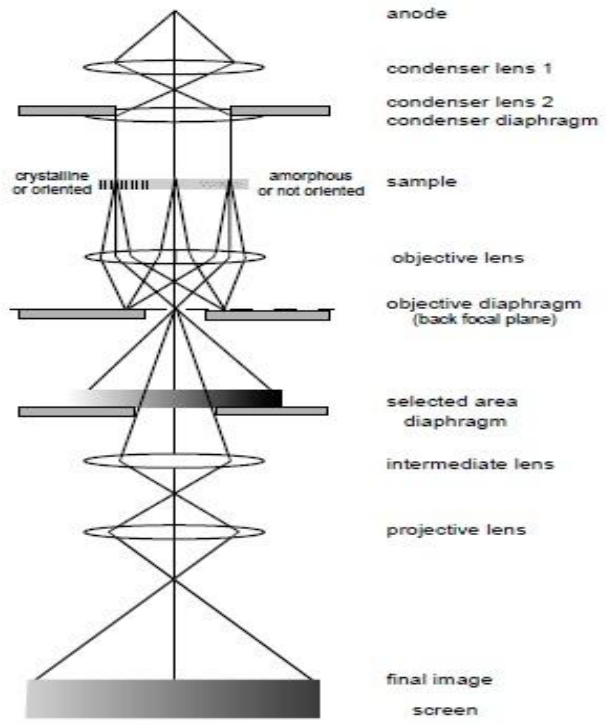

Figure 5.8. Schematic Diagram of TEM[73]

Figure 5.9. Picture of TEM set up @JNU

(A) Imaging mode

If the sample is thin (< 200 nm) and made up of early periodic table chemical elements, the image presents a very low contrast when it is focused. To get an amplitude contrasted image, an objective diaphragm has to be inserted in the back focal plane to select the transmitted beam (and possibly few diffracted beam): the crystalline parts in Bragg orientation appears to be dark and not Bragg oriented parts or the amorphous appear bright. This type of imaging mode is called *bright field* mode BF. If the diffraction is made up of many diffracting phases, each of them can individually be differentiated by selecting one of its diffracted beams with the help of objective diaphragm. To do so, the incident beam must be angled so that the diffracted beam is put on the objective lens axis to avoid off axis aberrations . This mode is known as *dark field* mode DF. The bright field and dark field modes are used for imaging materials to nanometer scale.

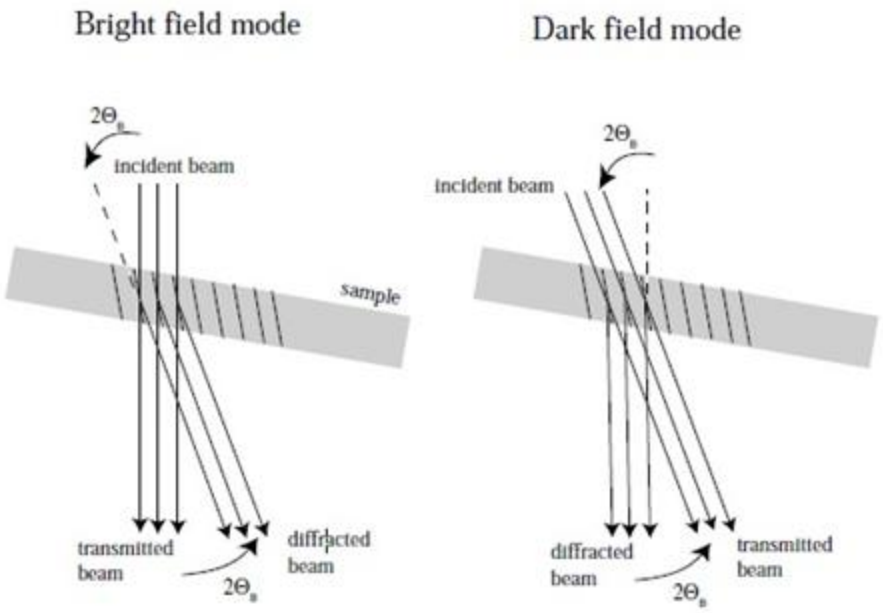

Figure 5.10. Bright and dark field modes for imaging[74]

(B) Diffraction Modes

The selected area diaphragm is used only to select one part of imaged sample for example a particle or a precipitate. This mode is known as selected area diffraction SAED. The spherical aberrations of the objective lens restrict the area of the selected object to few hundreds of

nanometers. However, it is possible to obtain diffraction patterns of a smaller object by focusing the electron beam with the projector lenses to obtain a small spot size on the object surface (2-10 nm). The spots of SAED become disks whose radii depend on the condenser diaphragm. This is called microdiffraction.

SAED and microdiffraction patterns of a crystal permit to obtain the symmetry of its lattice and calculate its interplanar distances (with the Bragg law). This is useful to confirm the identification of a phase, after assumptions generally based on the literature of the studied system and on chemical analyses.

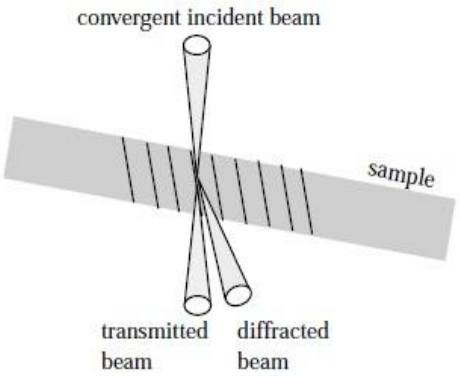

Figure 5.11. Diffraction Mode[75]

6. Results and Discussions

In order to check for the structural measures of synthesized Ni filled carbon nanotube various characterization tools are used as discussed in previous chapter, here in this particular chapter we will focus on the obtained results in the form of images(in the case of SEM and TEM) as well as results obtained in the form of curve/graph(in the case of XRD and Raman Spectroscopy) and the interpretation of the results.

6.1 X Ray Diffraction

Here in Advance Instrumentation centre at DTU, we have BRUKER D8 ADVANCED and the same has been used to carry on the characterization of Ni filled CNTs. The XRD pattern of the Ni filled CNTs prepared through Thermal CVD using Nickelocene as a catalyst is indicated in Fig. 6.1. The strongest peaks of the CNTs correspond to the plane of (0 0 2) of graphite, which indicates that the CNTs are with a very high ordering of the graphitic layers. Whereas other peaks are indexed as the plane of (1 1 1), (2 0 0) and (2 2 0) of metallic Ni with fcc structure. In addition, there is no nickelocene of the cementite phase detected, which was also identified in Ni-filled carbon nanocaps. The diffraction peaks in the 20° to 80° can be indexed as Ni (111), (200), and (220), which belong to the fcc structure, and C (002), which belong to the graphitic structure.

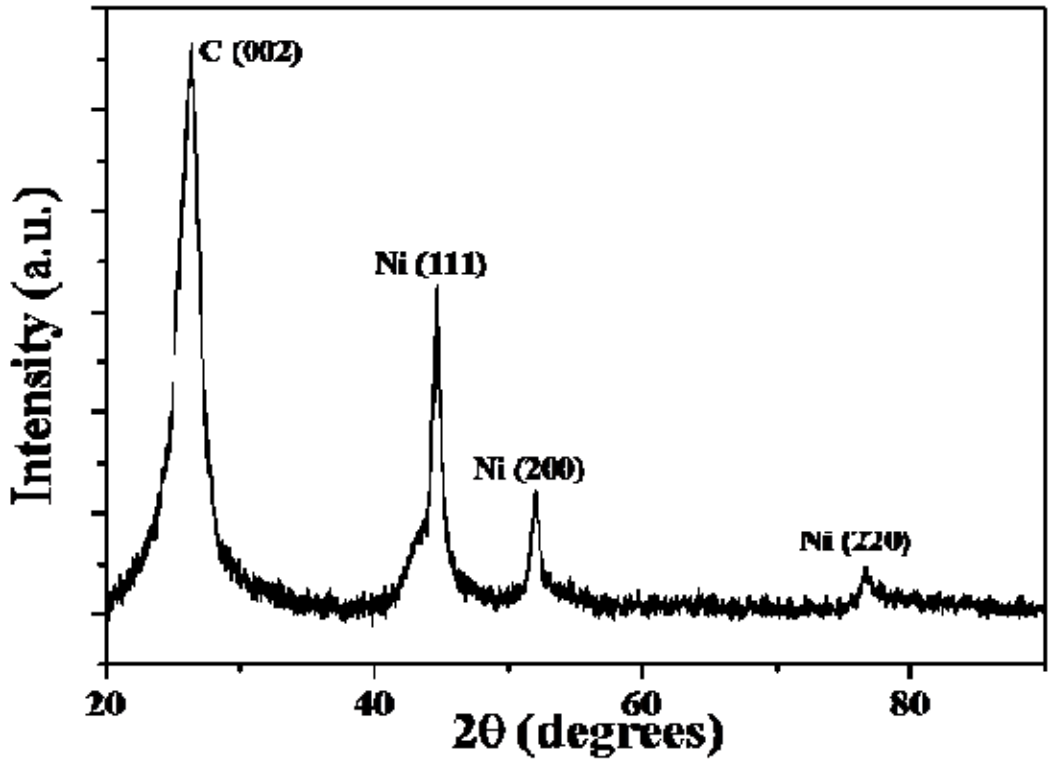

Figure 6.1. X Ray Diffraction pattern of the as-obtained sample

6.2 Scanning Electron Microscopy

As I have considered SEM to be the preliminary characterization tool which means the synthesized sample is firstly viewed in SEM in order to see whether the yield of grown sample is good or not and only if good yield is confirmed further characterization is performed. Optization process as discussed in previous chapter which dealt with parameters like temperature, precursor concentration and gas flow and their impact on the yield can be seen clearly in the various SEM images to be follow.

Here in Advance Instrumentation Centre at DTU, we have HITACHI S3700N and the same has been used to carry on the characterization of Ni filled CNTs.

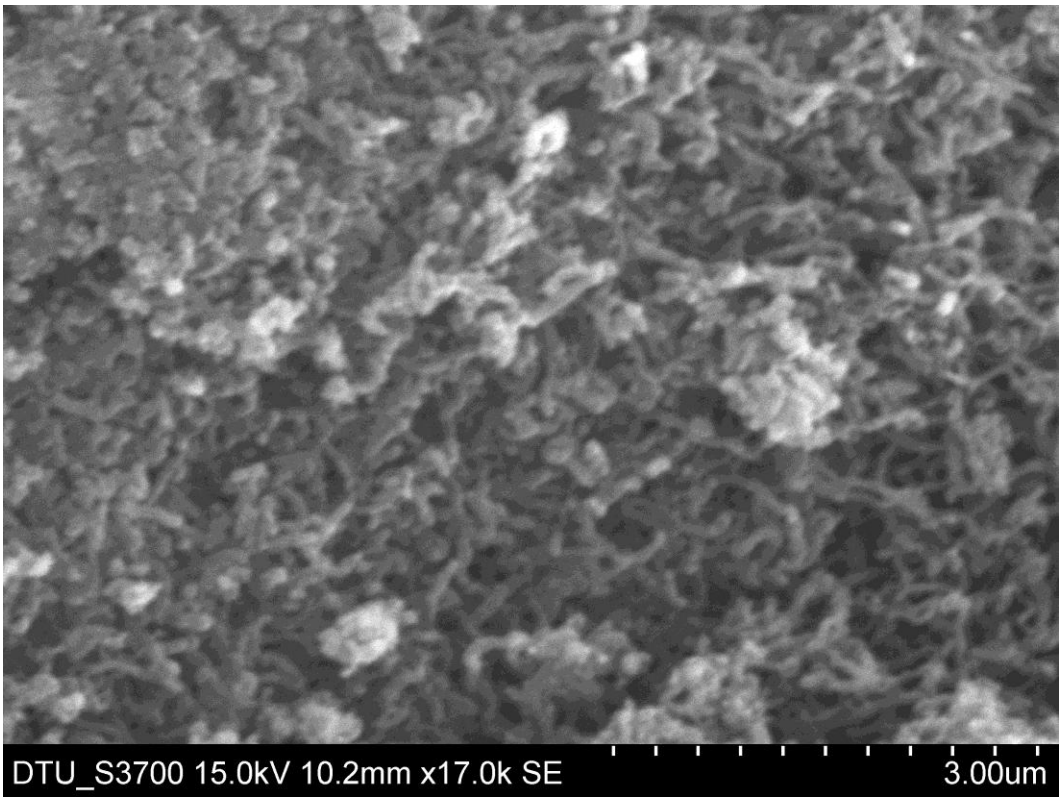

Figure 6.2. SEM image of the as-obtained sample

The above obtained image is corresponding to the concentration of Benzene to be 20 ml and Nickelocene to be 0.2 gm. As it is evident from the above image that the formation of CNT is definitely there but the yield seems on the lower side as there is a lot of bulk and also the uniformity of the obtained sample is not up to the standard. So in order to eliminate these two drawbacks some of the synthesis parameters has to be altered. Taking concentration to be the first parameter as the obtained sample yield is very low which mean there is excess of Benzene present.

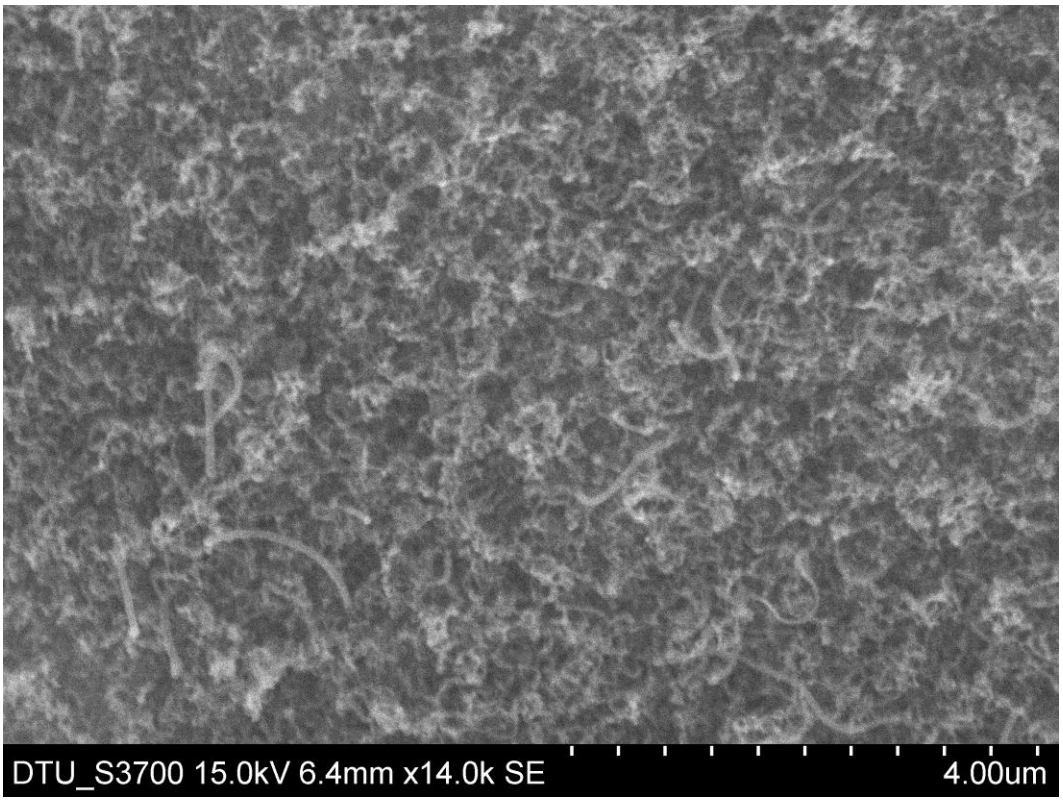

Figure 6.3. SEM image of the as-obtained sample

This SEM image corresponds to the concentration of Benzene to be 10 ml and Nickelocene to be 0.2 gm as it is clearly deducible that yield as well as uniformity of the obtained sample has increased drastically. The yield has been calculated as follows, the obtained sample weight(let it be X) is divided by Nickelocene weight(let it be Y). To get percentage yield X/Y is multiplied by 100. So in this case yield came out to be 50%. But still there is room for increment in yield moreover the uniformity can also be improved.

The next parameter taken in order to optimize is gas flow. All the above conducted experiment is carried out at flow rate of 150 sccm for argon and 50 sccm for hydrogen but as observed in the case of iron filled CNT only hydrogen is able to carry out the reaction so here only hydrogen is passed through the tube at a constant rate of 50 sccm. But as we can see below in the SEM image that neither it helped in yield as there is negligible yield nor it helped on the uniformity front so this method was discarded but the problem in hand is still there as yet we have not been able to optimize the flow parameter. So this time instead of flowing both the gases simultaneously what

we did was that argon is allowed to pass into the tube 5 min earlier than hydrogen and the results were improved.

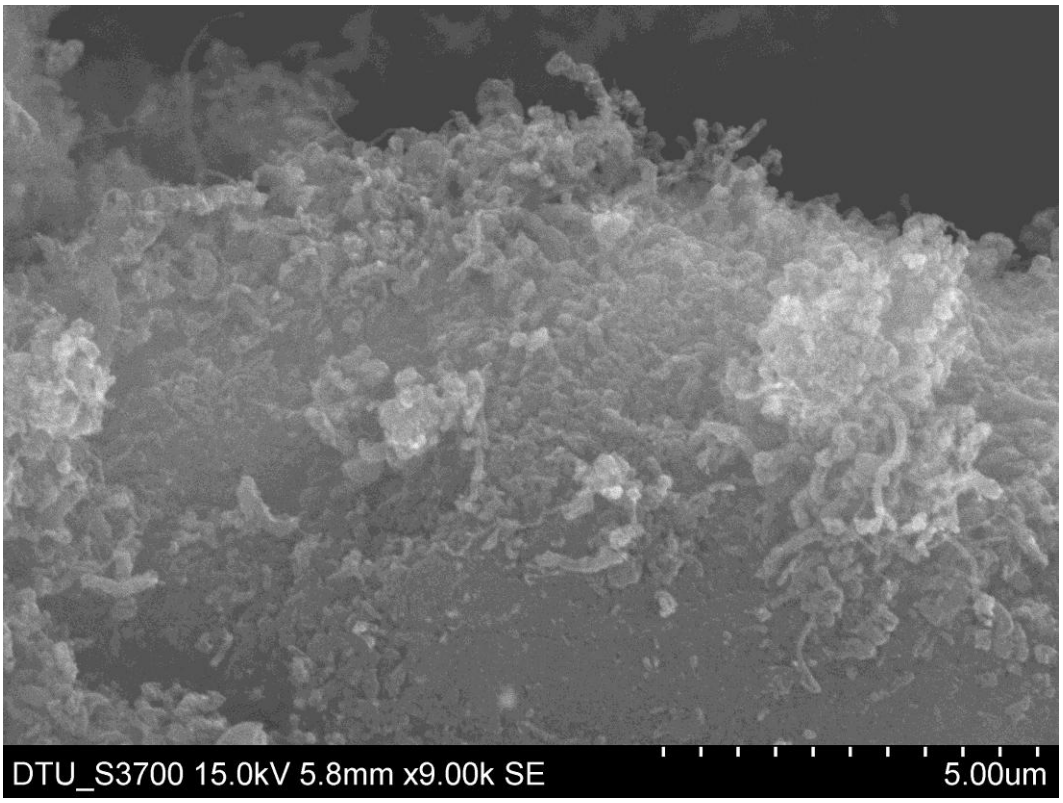

Figure 6.4. SEM image of the as-obtained sample

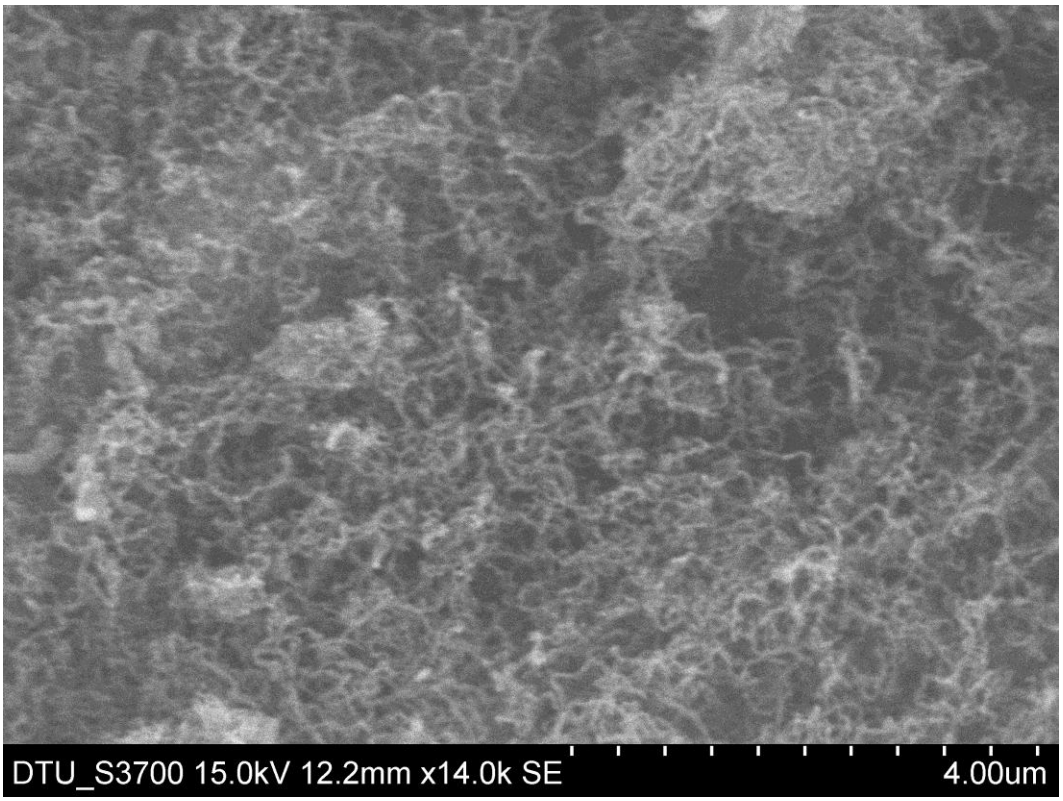

Figure 6.5. SEM image of the as-obtained sample

Here for this sample the uniformity is clearly better than the previous attempts and also the yiels is increased. As for now we have optimized the flow rate and concentration but temperature is yet to be optimized which has been from room temperature to 850 ℃.

The following images are of sample which is synthesized under the above two optimized value of flow rate and concentration and keeping the temperature a little low this time as it has been increased from room temperature to 820 ℃.

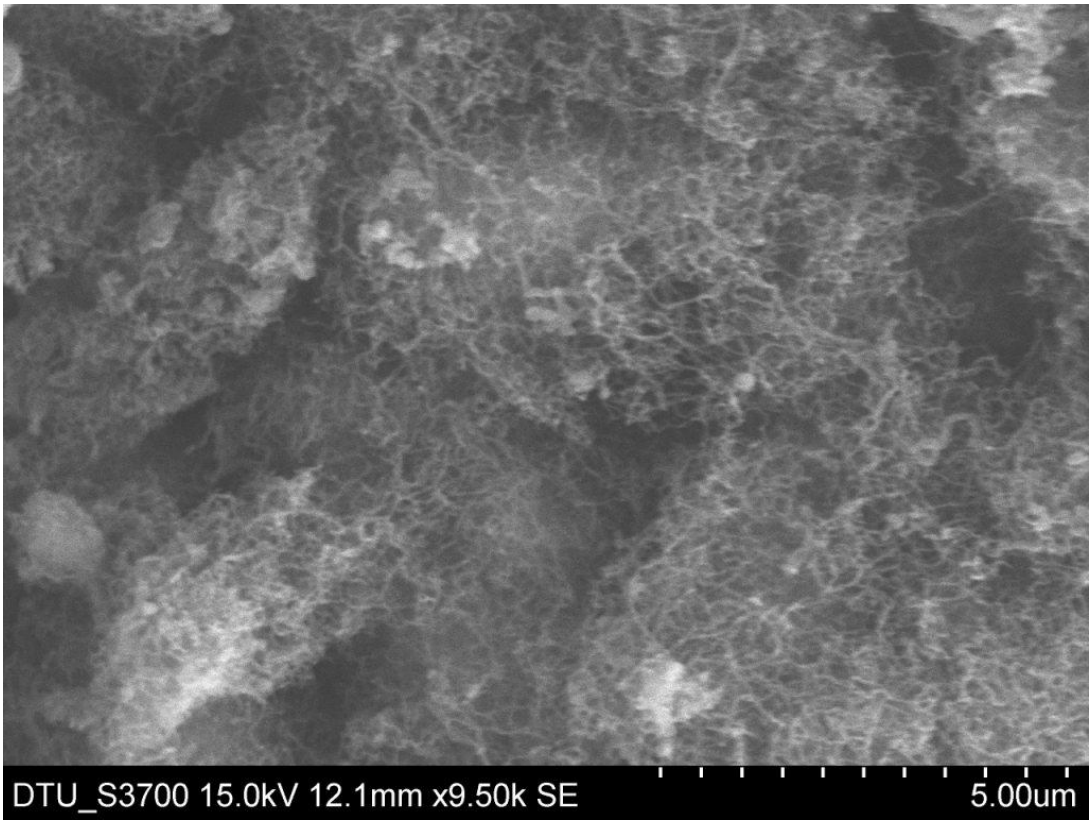

Figure 6.6. SEM image of the as-obtained sample

By calculating the yield this time which came out to be more than 100% and further varying the temperature it has been deduced that along with the previous two optimized parameter, temperature has also been optimized at 820 °C. Some more images of the considered optimized sample are given below.

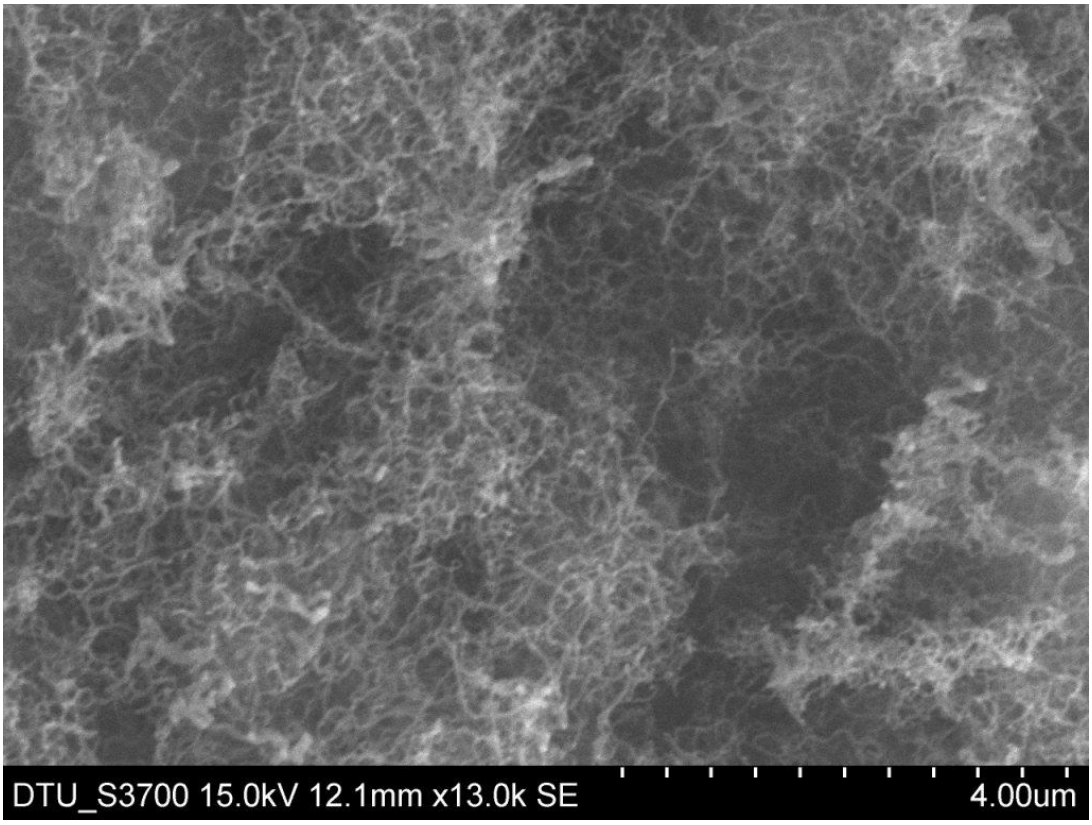

Figure 6.7. SEM image of the as-obtained sample

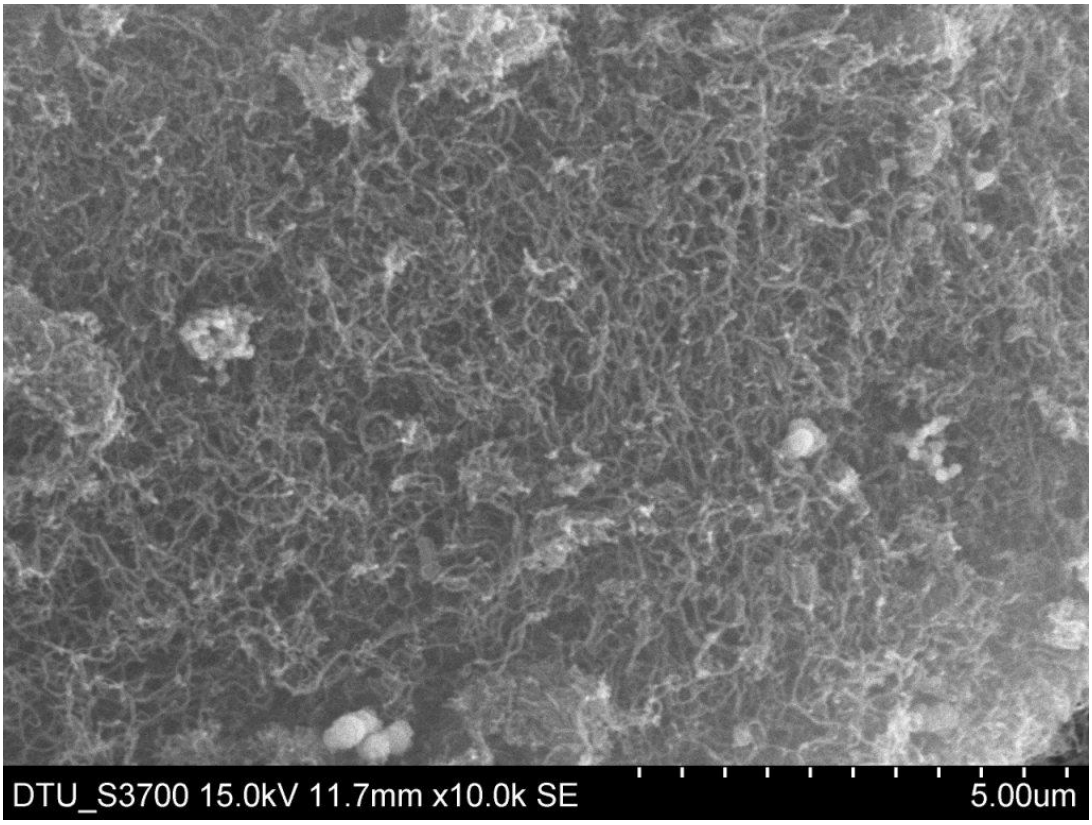

Figure 6.8. SEM image of the as-obtained sample

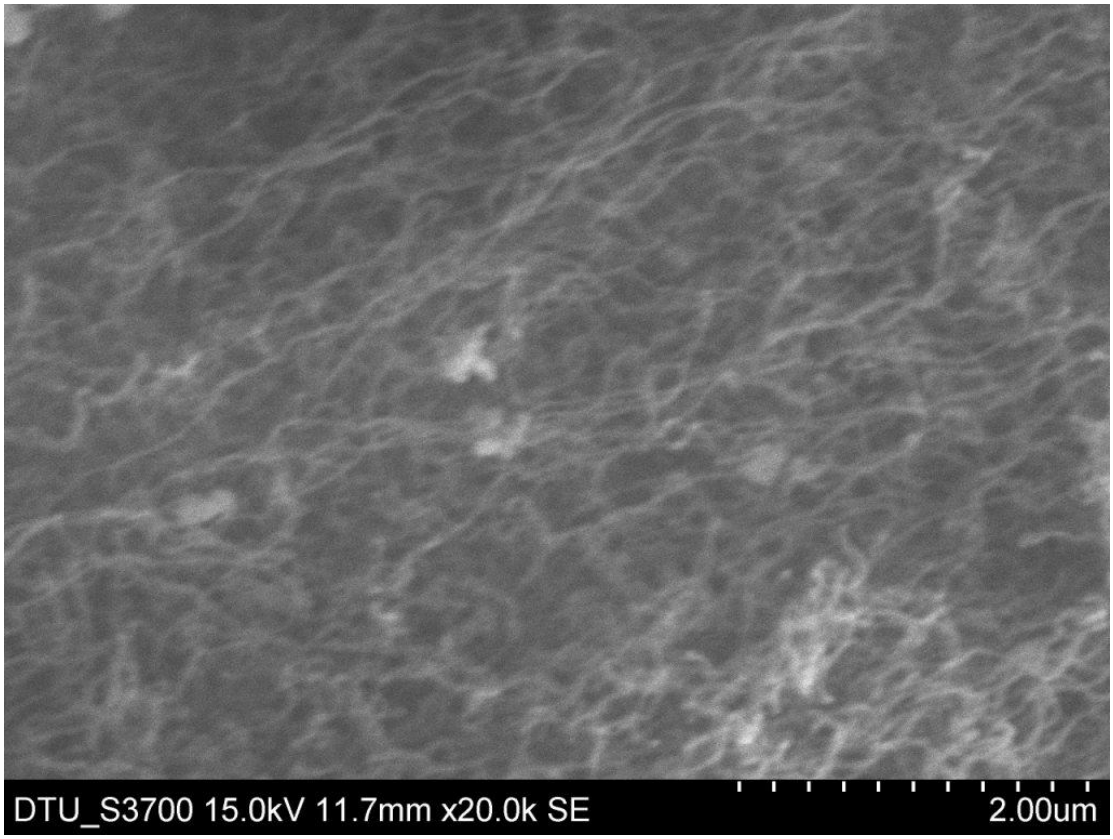

Figure 6.9. SEM image of the as-obtained sample

6.3 Raman Spectroscopy

Information about the crystallinity of bulk material can be measured by Raman spectroscopy. Raman spectra of sample grown at optimized conditions that is all three parameters(temperature, concentration and gas flow) were kept in accordance with the above findings is shown in the figure below. For Ni filled CNT, the active tangential mode (G-line) is found around 1600 inverse cm, which results from the E2g-mode of graphite. In the case of a perfect crystalline structure only this line would be found. However, the defect-induced mode (D-line) around 1300 inverse cm is always found. This line results from a Raman double scattering process and is proportional to the defect density in the CNT. The peaks at a Raman shift of 1346 cm-1 (D band) and 1578 cm-1 (G band) are typical of MWNTs. The former is the so-called defect induced D band, whereas the latter is related to vibrations in all sp2 carbon materials. The intensity ratio of

the D band to the G band is ID/IG = 0.84, indicating a significant graphitization degree of the capsules. This characterization not only confirms about the crystallinity but also put down the fact that the formed CNTs are multi walled, i.e., MWNTs.

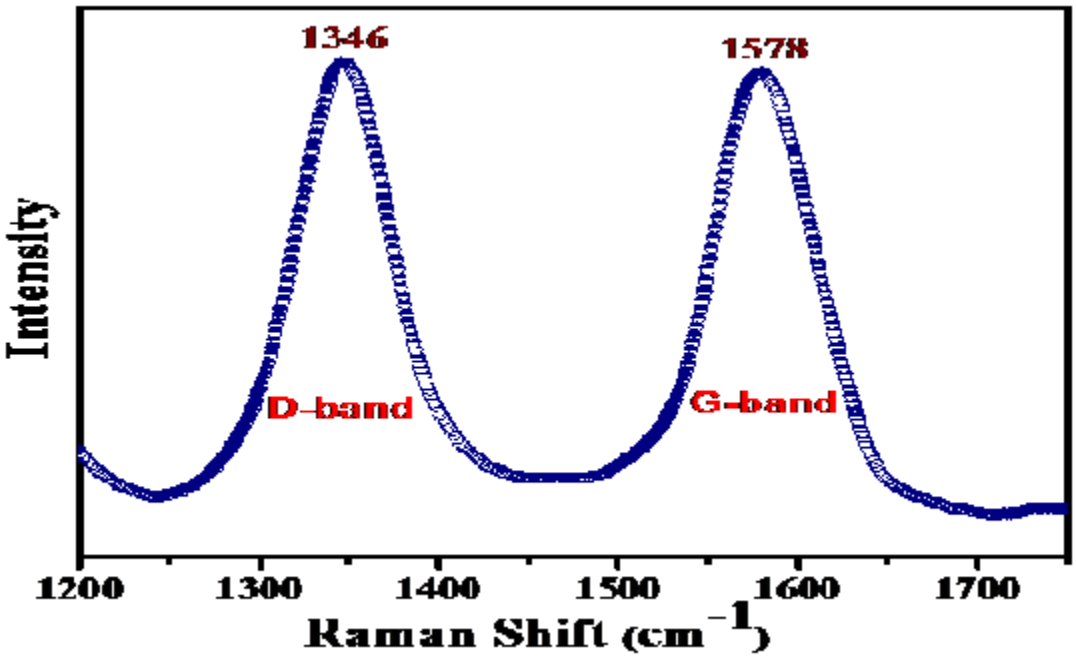

Figure 6.10. Raman Plot of the as-obtained sample

6.4 Transmission Electron Microscopy

TEM analysis of obtained sample of Ni filled CNT is carried out by JEOL 2100F at AIRF (Advanced Instrumentation Research Facility) in JNU. In order to focus more closely at the structure of the tubes, TEM studies has to be performed. This technique is predominately helpful in deducing the diameter of Ni filled CNTs as well as carries information about the filling. Below are some TEM images of as grown Ni filled CNTs, which are discussed under this heading.

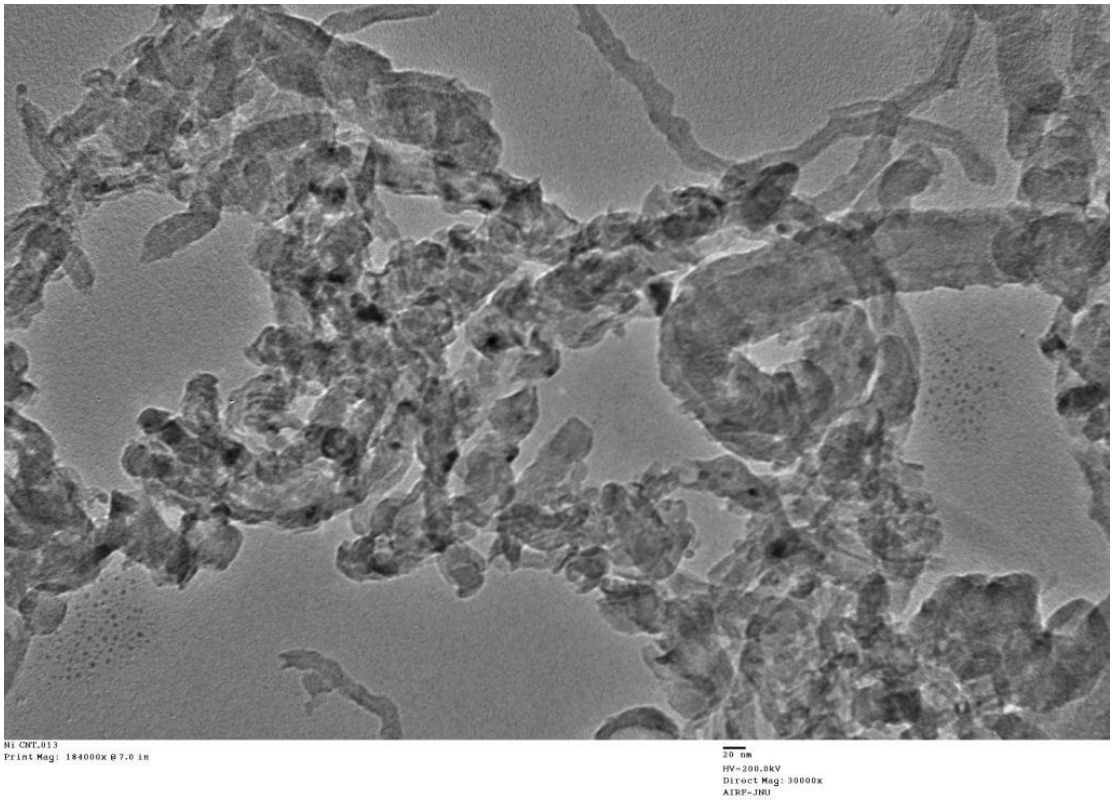

Figure 6.11. TEM image of the as-obtained sample

The above image shows a bunch of as grown Ni filled CNTs, the dark spots represents the metallic filling of Ni, as it is evident from the image that filling is found to be non linear and somewhat beads like filling is observed.

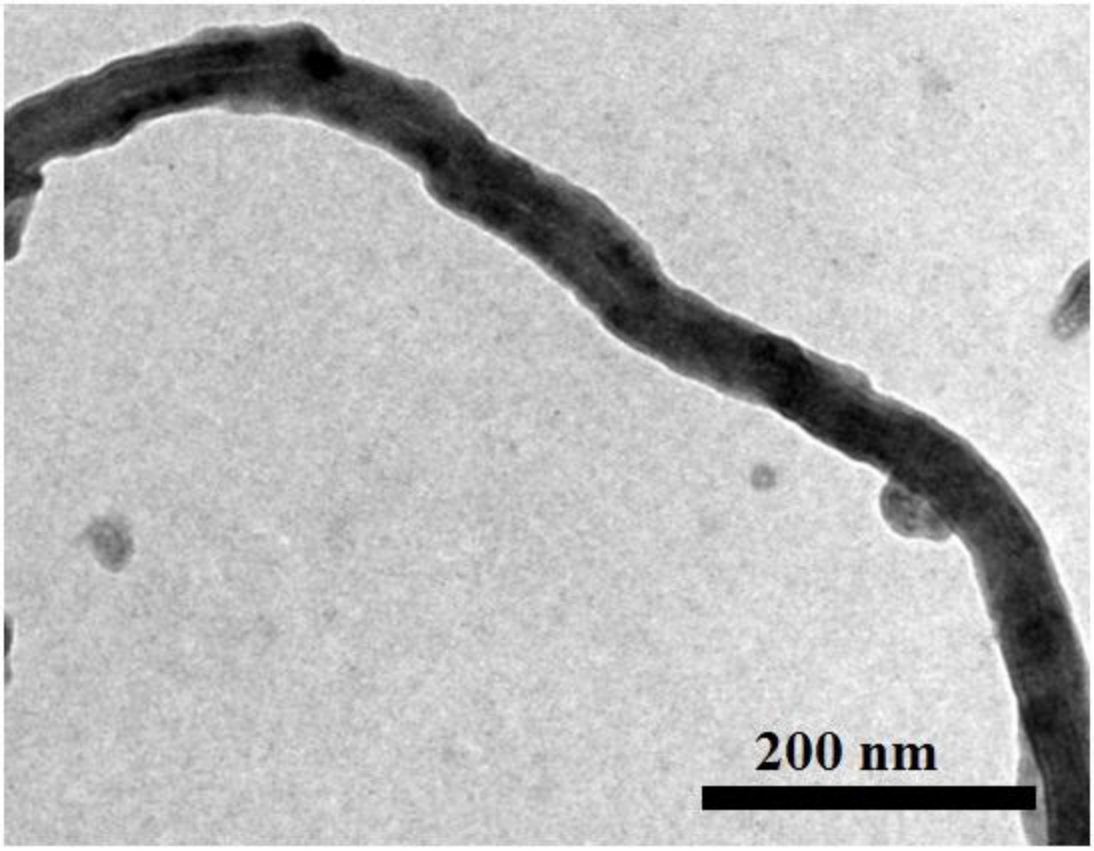

Figure 6.12. TEM image of the as-obtained sample

The above image is of a single strand of as grown Ni filled CNT, here filling can be seen clearly at the tip of CNT. More filling is observed in the following images given below.

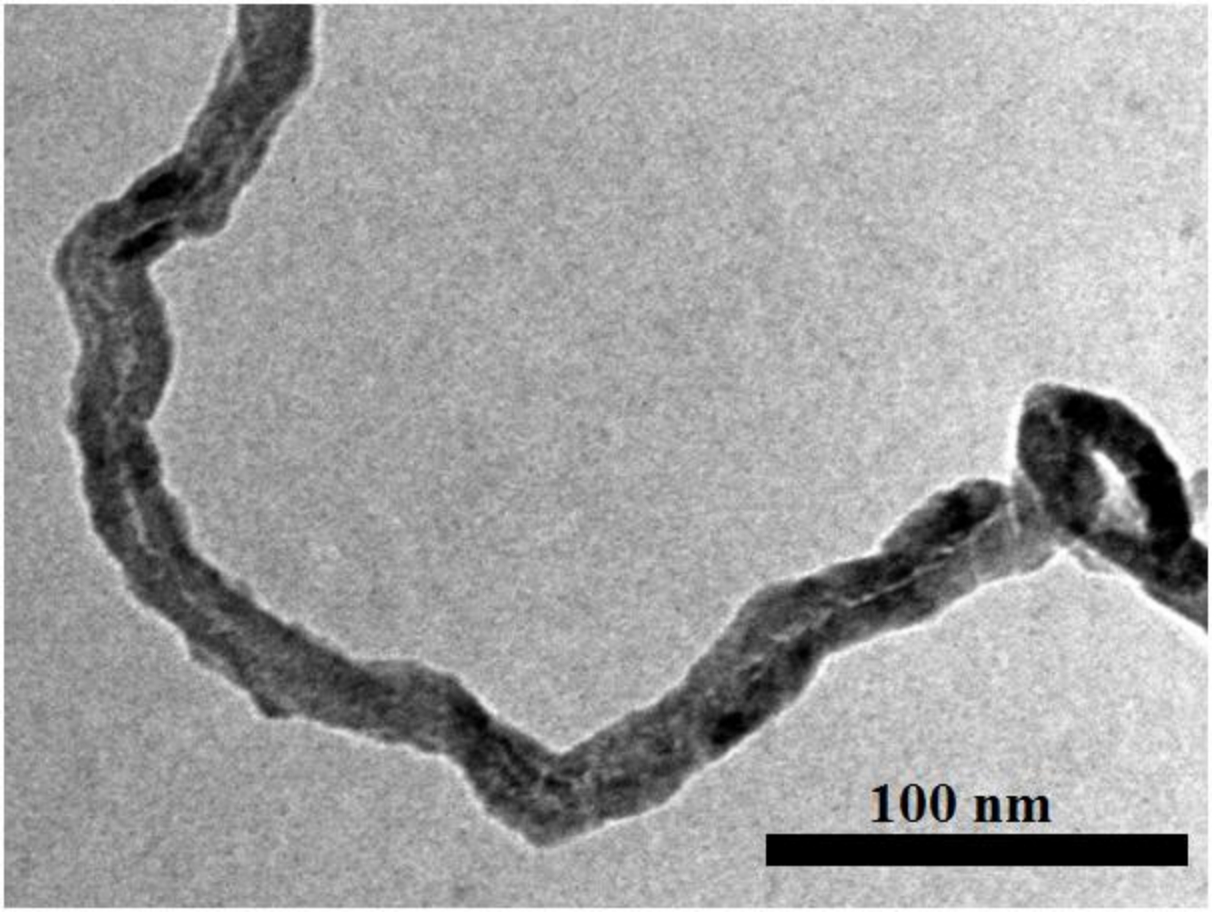

Figure 6.13. TEM image of the as-obtained sample

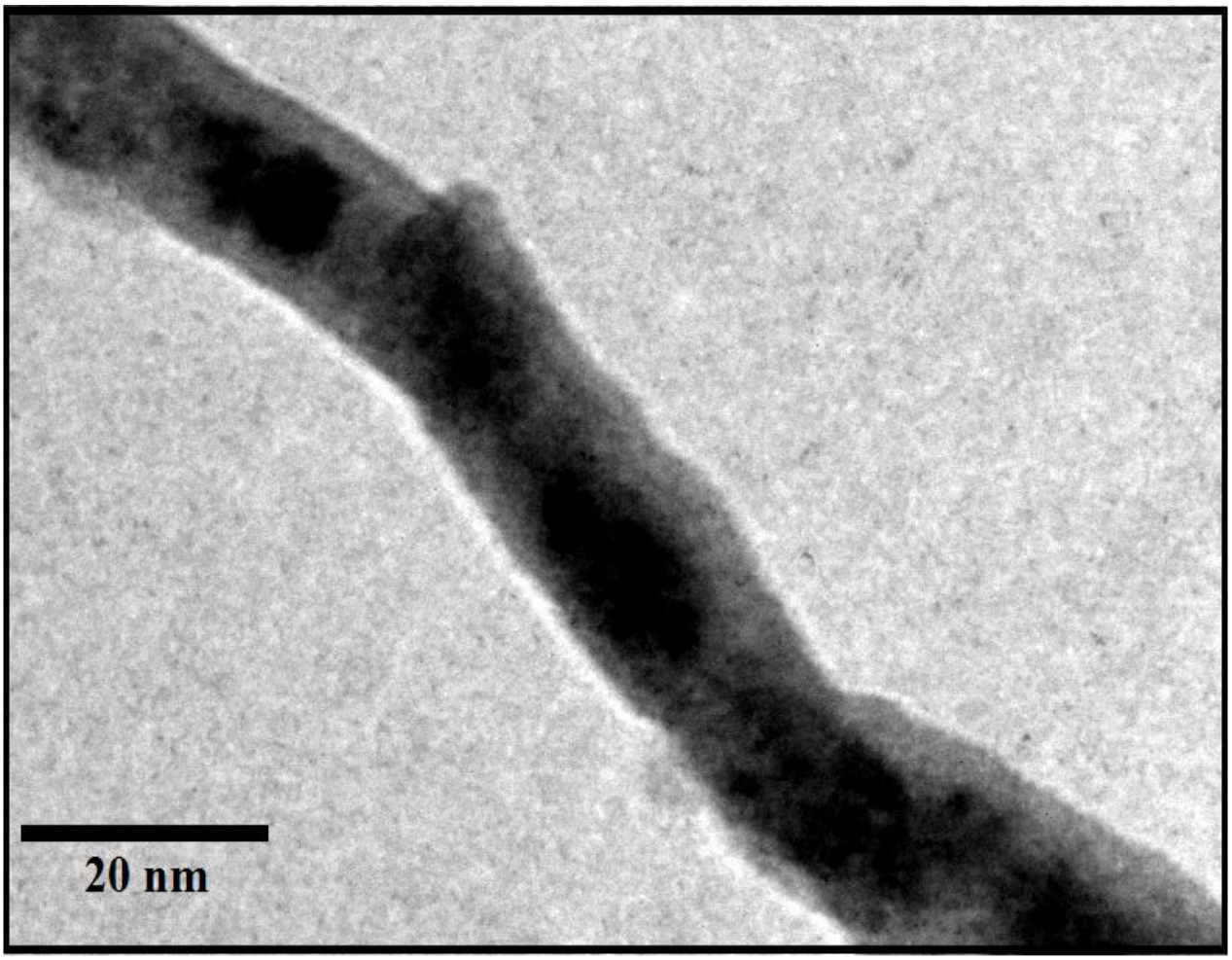

Figure 6.14. TEM image of the as-obtained sample

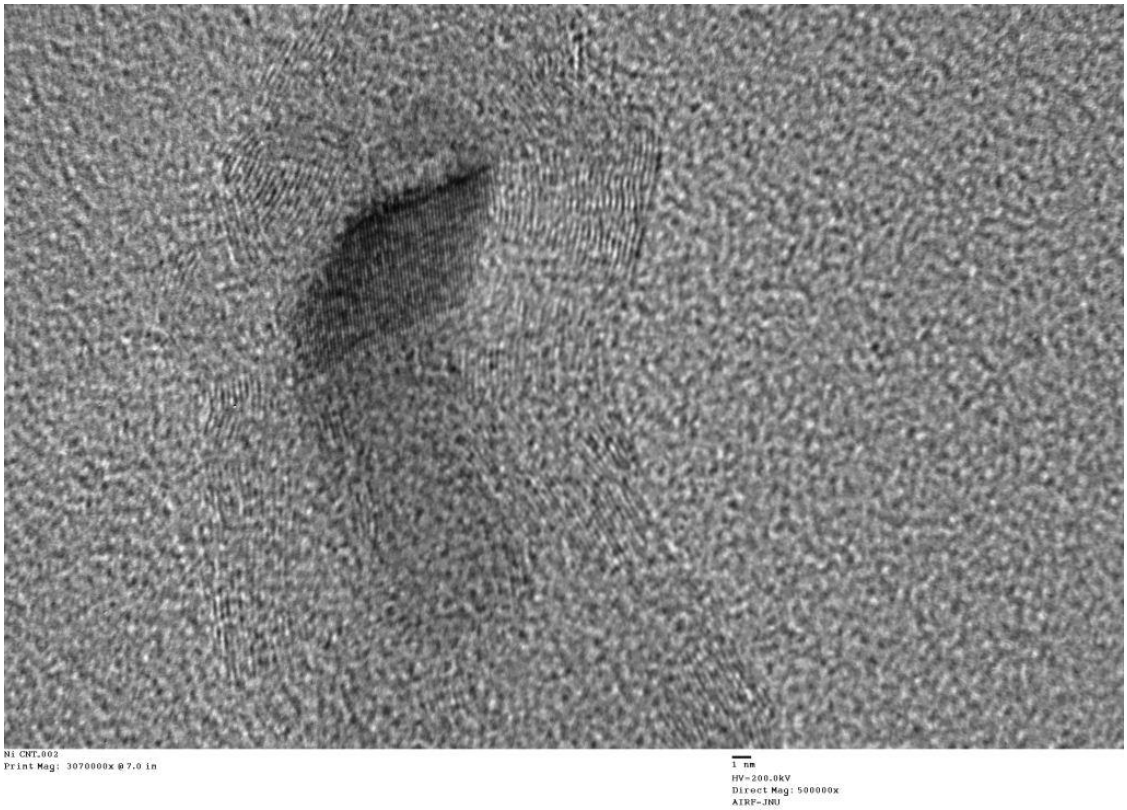

Figure 6.15. TEM image of the as-obtained sample

This a HRTEM image taken at a very high magnification it clearly shows the lattice and it is evident that the synthesized CNTs are of multi walled in nature. The filling can be seen in between the walls of CNTs.

7. Conclusion

The objective of this project was to design as well as implement an optimized method for the growth of Ni-encapsulated carbon nanotubes using thermal CVD and to characterize it using standard available characterization techniques.

A chemical vapour deposition method was used as the synthesis route, within the means of the equipments available, in order to synthesize Ni-encapsulated carbon nanotubes. The conditions necessary for successful growth were thoroughly researched and experimentally fine tuned in order to achieve the desired reproducible growth of fairly large yield. A chemical mixture of 10 mL benzene and 0.2 gm of nickelocene were put inside the furnace with the gas flows of hydrogen and argon as 50 sccm and 150 sccm ,upto a temperature of 820 °C.
The resulting yield was measured to be 200%. Moreover, the standard characterization techniques also confirmed the quality and characteristics of the as-synthesized sample.

7.1 Future Work

Although carbon nanotubes have been the centre of attraction amongst researchers for these last few years, however, a method for consistent and reproducible growth that is feasible for commercial purpose is still far off, as experienced during the course of this project. Even though research is ongoing on the different arenas of usefulness of CNTs, still much more can be done in order to explore the full potential of this unique structure. Then the research could probably progress to the replacement of silicon by CNT in the semiconductor industry. This work could strongly pave the way to realization of 1D transistors in the near future. At the rate Moore's Law is progressing, by 2019 it will result in transistor just a few atoms in width. This means that the strategy of ever finer photolithography will have run its course; we have already seen a progression from a micron, to submicron to 45 nm scale. Carbon Nanotubes, whose walls are just 1 atom thick, with diameters of only 1 to 2 nm, seems to be one of the perfect candidates to take us right to the end of Moore's Law curve. We possibly cannot go beyond that. So certainly, Carbon Nanotubes have a promising future.

8. References

1. Anthuvan Rajesh John, Pandurangan Arumugam. Studies on structural and magnetic properties of pristine and nickel-filled carbon nanotubes synthesized using LaNi5 alloyparticles as a catalyst. *Chemical Engineering Journal 243 (2014) 436–447*
2. Uhland Weissker , Silke Hampel, Albrecht Leonhardt, Bernd Buchner. Carbon Nanotubes Filled with Ferromagnetic Materials. *Materials 2010, 3, 4387-4427*
3. D. Ostling, D. Tomanek, A. Rosen. Electronic structure of single-wall, multiwall, and filled carbon nanotubes. *1997 The American Physical Society, 0163-1829/97/55(20)/13980~9*
4. M. Monthioux. Filling single-wall carbon nanotubes. *Carbon 40 (2002) 1809 –1823*
5. Vıctor M. Garcıa-Suarez , Jaime Ferrer , Colin J. Lambert. Tuning the electrical conductivity of nanotube-encapsulated metallocene wires.
6. H. Kataura, Y. Kumazawa , Y. Maniwa , I. Umezu , S. Suzuki , Y. Ohtsuka, Y. Achiba. Optical Properties of Single Wall Carbon Nanotubes. *Synthetic Metals 103 (1999) 2555-2558*
7. Jianchun Bao,Quanfa Zhou, Jianming Hong,Zheng Xu.Synthesis and magnetic behavior of an array of nickel-filled carbon nanotubes. *Appl. Phys. Lett., Vol. 81, No. 24, 9 December 2002*
8. RAJASHREE HIRLEKAR, MANOHAR YAMAGAR, HARSHAL GARSE, MOHIT VIJ, VILASRAO KADAM. CARBON NANOTUBES AND ITS APPLICATIONS: A REVIEW. *Asian Journal of Pharmaceutical and Clinical Research. Vol.2 Issue 4, October- December 2009.*
9. M A Zeeshan, K Shou, S Pané, E Pellicer, J Sort, K M Sivaraman, M D Baró, B J Nelson. Structural and magnetic characterization of batch fabricated nickel encapsulated multi-walled carbon nanotubes.
10. Ferenc Stercel,Norbert M. Nemes, John E. Fischer,David E. Luzzi. Single Wall Carbon Nanotubes Filled with Metallocenes: a First Example of Non-Fullerene Peapods. *Materials Research Society.*
11. Uhland Weissker, Silke Hampel, Albrecht Leonhardt and Bernd Buchner. Carbon Nanotubes Filled with Ferromagnetic Materials. *Materials 2010, 3, 4387-4427; doi:10.3390/ma3084387.*
12. G. Che, B. B. Lakshmi, C. R. Martin, E. R. Fisher, Rodney S. Ruoff. Chemical Vapor Deposition Based Synthesis of Carbon Nanotubes and Nanofibers Using a Template Method. *Chem. Mater.* **1998,** *10,* 260-267.
13. A. Leonhardt , M. Ritschel, R. Kozhuharovaa, A. Graffa, T. Muhl, R. Huhle, I. Monch, D. Elefant, C.M. Schneider. Synthesis and properties of filled carbon nanotubes. *Diamond and Related Materials 12 (2003) 790–793*
14. Pawan K. Tyagi , M.K. Singh , Abha Misra , Umesh Palnitkar , D.S. Misra , E. Titus, N. Ali , G. Cabral , J. Gracio , M. Roy , S.K. Kulshreshtha. Preparation of Ni-filled carbon

nanotubes for key potential applications in nanotechnology. *Thin Solid Films 469–470 (2004) 127–130.*

15. Ajayan P M and Iijima S Capillarity induced *filling of carbon nanotubes*. 1993 Nature 361 333
16. Iijima, S.; Ichihashi, T. Single-shell carbon nanotubes of 1-nm diameter. Nature 1993,363, 603–605.
17. Ebbesen, T.W.; Ajayan, P.M. Large-scale synthesis of carbon nanotubes. Nature 1992, 358, 220.
18. Thess, A.; Lee, R.; Nikolaev, P.; Dai, H.; Petit, P.; Robert, J.; Xu, C.; Lee, Y.H.; Kim, G.S.; Rinzler, A.G.; Colbert, D.T.; Scuseria, G.; Tomanek, D.; Fischer, J.E.; Smalley, R.E. Crystalline Ropes of Metallic Carbon Nanotubes. Science 1996, 273, 483–487.
19. Jos_e-Yacam_an, M.; Miki-Yoshida, M.; Rend_on, L.; Santiesteban, J.G. Catalytic growth of carbon microtubules with fullerene structure. Appl. Phys. Lett. 1993, 62, 657–659.
20. Moisala, A.; Nasibulin, A.G.; Kauppinen, E.I. The role of metal nanoparticles in the catalytic production of single-walled carbon nanotubes - a review. J. Phys.: Condens. Matter 2003,15, S3011–S3035.
21. Melechko, A.V.; Merkulov, V.I.; McKnight, T.E.; Guillorn, M.A.; Klein, K.L.; Lowndes, D.H.;Simpson, M.L. Vertically aligned carbon nanofibers and related structures: Controlled synthesis and directed assembly. J. Appl. Phys. 2005, 97, 041301–041339.
22. Leonhardt, A.; Hampel, S.; M¨uller, C.; M¨onch, I.; Koseva, R.; Ritschel, M.; Elefant, D.;Biedermann, K.; B¨uchner, B. Synthesis, Properties, and Applications of Ferromagnetic-Filled Carbon Nanotubes. Chem. Vap. Deposition 2006, 12, 380–387.
23. Saito, R.; Dresselhaus, G.; Dresselhaus, M.S. Physical Properties of Carbon Nanotubes; Imperial College Press: London, UK, 1998.
24. Thostenson, E.T.; Ren, Z.; Chou, T.W. Advances in the science and technology of carbon nanotubes and their composites: A review. Compos. Sci. Technol. 2001, 61, 1899–1912.
25. Tsang, S.C.; Chen, Y.K.; Harris, P.J.F.; Green, M.L.H. A simple chemical method of opening and filling carbon nanotubes. Nature 1994, 372, 159–162.

26. Hampel, S.; Leonhardt, A.; Selbmann, D.; Biedermann, K.; Elefant, D.; M¨uller, C.; Gemming, T.;B¨uchner, B. Growth and characterization of filled carbon nanotubes with ferromagnetic properties. Carbon 2006, 44, 2316–2322.
27. Kozhuharova, R.; Ritschel, M.; M¨onch, I.; M¨uhl, T.; Leonhardt, A. Selective Growth of Aligned Co-Filled Carbon Nanotubes on Silicon Substrates. Fuller. Nanotub. Carbon Nanostr. 2005,13, 347–353.
28. Monthioux, M. Filling single-wall carbon nanotubes. Carbon 2002, 40, 1809–1823.
29. Tasis, D.; Tagmatarchis, N.; Bianco, A.; Prato, M. Chemistry of carbon nanotubes. Chem. Rev. 2006, 106, 1105–1136.
30. Leonhardt, A.; M¨onch, I.; Meye, A.; Hampel, S.; B¨uchner, B. Synthesis of ferromagnetic filled carbon nanotubes and their biomedical application. Adv. Sci. Technol. 2006, 49, 74–78.
31. Balasubramanian, K.; Burghard, M. Chemically Functionalized Carbon Nanotubes. Small 2005,1, 180–192.
32. Klumpp, C.; Kostarelos, K.; Prato, M.; Bianco, A. Functionalized carbon nanotubes as emerging nanovectors for the delivery of therapeutics. Biochim. Biophys. Acta 2006, 1758, 404–412.
33. Tran, P.A.; Zhang, L.; Webster, T.J. Carbon nanofibers and carbon nanotubes in regenerative medicine. Adv. Drug Delivery Rev. 2009, 61, 1097–1114.
34. Bianco, A.; Kostarelos, K.; Prato, M. Applications of carbon nanotubes in drug delivery. Curr. Opin. Chem. Biol. 2005, 9, 674–679.
35. Klingeler, R.; Hampel, S.; Buechner, B. Carbon nanotube based biomedical agents for heating, temperature sensoring and drug delivery. Int. J. Hyperther. 2008, 24, 496–505.
36. Hilder, T.A.; Hill, J.M. Modeling the Loading and Unloading of Drugs into Nanotubes. Small 2009, 5, 300–308.
37. Kostarelos, K.; Bianco, A.; Prato, M. Promises, facts and challenges for carbon nanotubes in imaging and therapeutics. Nat. Nanotechnol. 2009, 4, 627–633.
38. M¨onch, I.; Meye, A.; Leonhardt, A.; Kr¨amer, K.; Kozhuharova, R.; Gemming, T.; Wirth, M.; B¨uchner, B. Ferromagnetic filled carbon nanotubes and nanoparticles: synthesis and lipid-mediated delivery into human tumor cells. J. Magn. Magn. Mater. 2005, 290/291, 276–278.

39. Kostarelos, K.; Lacerda, L.; Pastorin, G. Cellular uptake of functionalized carbon nanotubes is independent of functional group and cell type. Nat. Nanotechnol. 2007, 2, 108–113.
40. Jin, H.; Heller, D.A.; Strano, M.S. Single-Particle Tracking of Endocytosis and Exocytosis of Single-Walled Carbon Nanotubes in NIH-3T3 Cells. Nano Lett. 2008, 8, 1577–1585.
41. Son, S.J.; Bai, X.; Nan, A.; Ghandehari, H.; Lee, S.B. Template synthesis of multifunctional nanotubes for controlled release. J. Contr. Rel. 2006, 114, 143–152.
42. Lacerda, L.; Bianco, A.; Prato, M.; Kostarelos, K. Carbon nanotubes as nanomedicines: From toxicology to pharmacology. J. Contr. Rel. 2006, 58, 1460–1470.
43. Ajayan, P.M.; Iijima, S. Capillarity-induced filling of carbon nanotubes. Nature 1993, 361, 333–334.
44. Bao, J.; Zhou, Q.; Hong, J.; Xu, Z. Synthesis and magnetic behavior of an array of nickel-filled carbon nanotubes. Appl. Phys. Lett. 2002, 81, 4592–4594.
45. Dyagileva, L.M.; Mar'in, V.P.; Tsyganova, E.I.; Razuvaev, G.A. Reactivity of the first transition row metallocenes in thermal decomposition reaction. J. Organomet. Chem. 1979, 175, 63–72.
46. M¨uller, C.; Golberg, D.; Leonhardt, A.; Hampel, S.; B¨uchner, B. Growth studies, TEM and XRD investigations of iron-filled carbon nanotubes. Phys. Status Solidi A 2006, 203, 1064–1068.
47. Andrews, R.; Jacques, D.; Rao, A.M.; Derbyshire, F.; Qian, D.; Fan, X.; Dickey, E.C.; Chen, J. Continuous production of aligned carbon nanotubes: a step closer to commercial realization. Chem. Phys. Lett. 1999, 303, 467–474.
48. Kamalakaran, R.; Terrones, M.; Seeger, T.; Kohler-Redlich, P.; R¨uhle, M.; Kim, Y.A.; Hayashi, T.; Endo, M. Synthesis of thick and crystalline nanotube arrays by spray pyrolysis. Appl. Phys. Lett. 2000, 77, 3385–3387.
49. Zhang, X.; Cao, A.; Wei, B.; Li, Y.; Wei, J.; Xu, C.; Wu, D. Rapid growth of well-aligned carbon nanotube arrays. Chem. Phys. Lett. 2002, 362, 285–290.
50. Deck, C. Vecchio, K. Growth of Well-Aligned Carbon Nanotube Structures in Successive Layers. J. Phys. Chem. B 2005, 109, 12353–12357.
51. www.nanocomptech.com/what-are-carbonnaotubes.

52. www.nanocomptech.com/what-are-carbonnaotubes/geometry.
53. www.nanocomptech.com/what-are-carbonnaotubes/history
54. www.nanocomptech.com/what-are-carbonnaotubes/history
55. https://en.wikipedia.org/wiki/Nickelocene
56. UhlandWeissker, Silke Hampel, Albrecht Leonhardt and Bernd B¨uchner, Carbon Nanotubes Filled with Ferromagnetic Materials.
57. UhlandWeissker, Silke Hampel, Albrecht Leonhardt and Bernd B¨uchner, Carbon Nanotubes Filled with Ferromagnetic Materials.
58. UhlandWeissker, Silke Hampel, Albrecht Leonhardt and Bernd B¨uchner, Carbon Nanotubes Filled with Ferromagnetic Materials.
59. UhlandWeissker, Silke Hampel, Albrecht Leonhardt and Bernd B¨uchner, Carbon Nanotubes Filled with Ferromagnetic Materials.
60. UhlandWeissker, Silke Hampel, Albrecht Leonhardt and Bernd B¨uchner, Carbon Nanotubes Filled with Ferromagnetic Materials.
61. Nanotechnology: practices and principles by suelbha kulkarni.
62. Nanotechnology: practices and principles by suelbha kulkarni.
63. Nanotechnology: practices and principles by suelbha kulkarni.
64. Nanotechnology: practices and principles by suelbha kulkarni.
65. UhlandWeissker, Silke Hampel, Albrecht Leonhardt and Bernd B¨uchner, Carbon Nanotubes Filled with Ferromagnetic Materials.
66. UhlandWeissker, Silke Hampel, Albrecht Leonhardt and Bernd B¨uchner, Carbon Nanotubes Filled with Ferromagnetic Materials.
67. UhlandWeissker, Silke Hampel, Albrecht Leonhardt and Bernd B¨uchner, Carbon Nanotubes Filled with Ferromagnetic Materials.
68. https://en.wikipedia.org/wiki/X-ray_crystallography
69. https://en.wikipedia.org/wiki/Scanning_electron_microscope
70. Nanotechnology:Practices and principle by sulebha kulakarni.
71. https://en.wikipedia.org/wiki/Raman_spectroscopy
72. Nanotechnology:Practices and principle by sulebha kulakarni
73. Nanotechnology:Practices and principle by sulebha kulakarni
74. Nanotechnology:Practices and principle by sulebha kulakarni